Mount Pinatubo's effect on the moisture-based drivers of plant productivity

Ram Singh^{1,2}, Kostas Tsigaridis^{1,2}, Diana Bull³, Laura P Swiler³, Benjamin M Wagman³, Kate Marvel²

Affiliations

- ¹ Center for Climate Systems Research, Columbia University, New York, USA
- ² NASA Goddard Institute for Space Studies, New York, NY-10025, USA
- ³ Sandia National Laboratories, Albuquerque, NM, USA

Correspondence: Ram Singh (<u>rs4068@columbia.edu</u>, <u>ram.bhari85@gmail.com</u>ram.bhari85@gmail.com)

15 Abstract

Large volcanic eruptions can significantly affect the state of the climate, including stratospheric sulfate concentrations, surface and top-of-atmosphere radiative fluxes, stratospheric and surface temperature, and regional hydroclimate. The prevalence of higher natural variability in how the regional rainfall respondsresponse to—the volcanic-induced climate perturbations creates a knowledge gap in our understanding of how eruptions affect ecohydrological conditions and plant productivity. Here, we will explore the understudied store (soil moisture) and flux (evapotranspiration) of water as the short-term ecohydrological control over plant productivity in response to the 1991 eruption of Mt. Pinatubo. We used the NASA's Earth system model for modeling of the 1991's-Mt. Pinatubo eruption and detection of detect the ensuing hydroclimate responseresponses. The model simulates a radiative perturbation of 5 Wm² and mean surface cooling of ~0.5 °C following the Mt. Pinatubo eruption in 1991. The rainfall response is spatially heterogeneous with large temporal variability, yet still shows suppressed rainfall in the northern hemisphere after the eruption. We find that up to 10-15% of land regions show a statistically significant agriculturally droclimate response. (wet and dry) as calculated by the Soil Moisture

Deficit Index (SMDI) and Evapotranspiration Deficit Index (ETDI). Results confirm that these higher order impacts impact metrics successfully present a more robust understanding of inferred plant productivity—impacts. Our results also explain the geographical dependence of various contributing factors to the compound response and their implications for exploring the climate impacts of such episodic forcings.

Introduction

30

31

32

33

34

35 36

37 38

39 40

41

42

43

44

45

46

47

48

49

50

51

52

53

54

Volcanic eruptions are the most prominent source of sulfate aerosols in the stratosphere and are among the natural drivers of climate variability. Volcanically-injected sulfate aerosols in the stratosphere alter the Earth's radiative balance by simultaneously reflecting incoming solar radiation and absorbing outgoing longwave radiation emitted from the Earth's surface (Robock, 2000). The presence of sulfate aerosol for months to years after an eruption and its microphysical transformation in the stratosphere affect the climate system through numerous direct and indirect effects (Barnes and Hofmann, 1997; Brad Adams et al., 2003; Briffa et al., 1998; Deshler et al., 2003; Lambert et al., 1993; LeGrande et al., 2016; LeGrande and Anchukaitis, 2015; Li et al., 2013; Pinto et al., 1989; Santer et al., 2014; Sigl et al., 2015; Singh et al., 2023; Tejedor et al., 2021; Toohey et al., 2019; Zambri et al., 2017; Zambri and Robock, 2016; Zhao et al., 1995). (Barnes and Hofmann, 1997; Briffa et al., 1998; Deshler et al., 2003; Kremser et al., 2016; LeGrande et al., 2016; Marshall et al., 2022; Tejedor et al., 2021; Timmreck, 2012; Toohey et al., 2019). The Mt. Pinatubo eruption (June 1991) remains the largest eruption in the satellite era, and it has been explicitly documented and analyzed for its radiative and climate impacts. Numerous studies based on satellite observations and supported through different modeling efforts estimated that Mt. Pinatubo injected 10-20 Tg of SO₂ at a range of 18-25 km of plume height (Aquila et al., 2012; Bluth et al., 1992; Dhomse et al., 2014; Gao et al., 2023; McGraw et

```
al., 2024; Mills et al., 2016; Sheng et al., 2015a, b; Stenchikov et al., 1998)(Aquila et al., 2012;
55
56
      Bluth et al., 1992; Dhomse et al., 2014; Gao et al., 2023; Sheng et al., 2015a, b; Stenchikov et al.,
      1998). The radiative impacts of Mt. Pinatubo's eruption estimate an aerosol optical depth of 0.15
57
58
      for 550 nm wavelength, with an effective radius in the range of 0.16 to 1 micrometer (µm) and
      net radiative forcing on the order of 5-6 Wm<sup>-2</sup> (Lacis et al., 1992; Sato et al., 1993; Stenchikov et
59
      al., 1998). (Lacis, 2015; Lacis et al., 1992; Sato et al., 1993; Stenchikov et al., 1998). Estimates of
60
      the induced surface cooling range between 0.3-0.7 °C; lower stratosphere warming estimates are
61
      in the range of 2-3 °C (Bluth et al., 1992; Dutton and Christy, 1992; Hansen et al., 1992;
62
      Labitzke and McCormick, 1992; Lacis et al., 1992; McCormick and Veiga, 1992; Minnis et al.,
63
64
      1993; Ramachandran et al., 2000; Stenchikov et al., 1998 Hansen et al., 1993).(Dutton and
65
      Christy, 1992; Hansen et al., 1992; Labitzke and McCormick, 1992; Lacis et al., 1992; Minnis et
66
      al., 1993; Ramachandran et al., 2000; Stenchikov et al., 1998).
67
             In this study, we aim to explore the mechanisms by which the Mt. Pinatubo eruption
68
      affected the hydroclimatic conditions and water-based drivers of plant productivity. Agricultural
69
      productivity is sensitive to changes in temperature and precipitation (Lobell and Field, 2007;
70
      Olesen and Bindi, 2002; Rosenzweig and Parry, 1994). Although much work has been devoted to
71
      understanding Mt. Pinatubo's impacts on plant productivity, the literature has been dominated by
72
      studies focusing on impacts from changes to the quantity and quality of incoming solar radiation
73
      (Farquhar and Roderick, 2003; Gu et al., 2002, 2003; Jones and Cox, 2001; Robock, 2005).
74
      Proctor et al. (2018) have estimated a decrease in C4 (maize) and C3 (soy, rice, and wheat)
75
      agricultural crop production in response to Mt. Pinatubo driven mainly by changes in incoming
      radiation. Krakauer and Randerson (2003) evaluated the role of surface cooling in reduced net
76
      primary productivity (NPP (Net Primary Productivity) using tree ring growth patterns following
77
```

multiple Mt. Pinatubo-sized eruptions in the last millennium record. Reduced NPP was found in northern mid to high latitudes, while the signal in the lower latitudes and tropics was either not significant insignificant or constrained by the other factors. Other studies have further expanded into societal impact research focusing on volcanically induced poorchanges to harvest and agricultural productivity over different regions (van Dijk et al., 2023; Hao et al., 2020; Huhtamaa and Helama, 2017; Manning et al., 2017; Singh et al., 2023; Toohey et al., 2016). Similarly, mucha plenty of work has been devoted to understanding the hydroclimate response to Mt. Pinatubo through changes in atmospheric precipitation (Barnes et al., 2016; Paik et al., 2020; Trenberth and Dai, 2007). Monsoon, as the monsoon seasonal rainfall decreases in the season after an following the eruption (Colose et al., 2016; Iles et al., 2013; Liu et al., 2016; Singh et al., 2023; Tejedor et al., 2021). It is also shown that volcanic eruptions can alter regional rainfall and hydroclimate in general, which could prominently affect regional plant productivity (Zuo et al., 2019a, b). However, rainfall alone provides an incomplete understanding of the drought conditions relevant forto plant productivity; a rainfall deficit could, in principle, be overcome by moisture stored in the soil.- Hence, meteorological drought indices (e.g. SPI (McKee et al., 1993) or PDSI (Palmer 1965)) based on rainfall ignore a full water balance approach. Furthermore, meteorological drought indices tend to be designed to evaluate prolonged periods of abnormally dry weather conditions. For instance, PDSI is an indicator of drought with a 9-month horizon (Mullapudi et al., 2023). (Mullapudi et al., 2023). Yet, agricultural crops are heterogeneously sensitive to the timing and degree of moisture deficits during particular portions of the crop growth cycle; for instance, corn yield can be decreased by

78

79

80

81

82

83

84

85

86

87

88

89

90

91

92

93

94

95

96

97

98

99

as much as 25% for a 10% water deficit during the pollination stage (Hane and Pumphrey, 1984).

Thus, consideration of indices with high temporal frequency can be especially important critical when focusing on agriculture. Soil moisture is the stock of water stored underground and is a primary source for the flux of water <u>flux</u> to the atmosphere and plants through evapotranspiration. Energetically, evaporation Evaporation of water from bare surface soil or transpiration of water during photosynthesis in plants from the root zone soils is demanding, using a dominantuses a large portion of absorbed solar energy (Trenberth et al., 2009). Plant transpiration is the largest contributor to land evapotranspiration (Nilson and Assmann, 2007; Seneviratne et al., 2010 and references therein). Soil moisture decrease in the root zone establishes an important(Dirmeyer et al., 2006; Lawrence et al., 2007; Nilson and Assmann, 2007; Seneviratne et al., 2010). Soil moisture decrease in the root zone establishes an essential control over plant productivity as transpiration is an integral component of photosynthesis (Chen and Coughenour, 2004; Denissen et al., 2022). Multiple studies have established that water supply is the limiting factor for climatic evapotranspiration over tropical and subtropical land areas, while temperature is an important controlling factor in northern mid- and high latitudes (Dong and Dai, 2017 and references therein). However, soil moisture changes in response to Mt. Pinatubo eruption (1991) are largely underreported in the literature(Dong and Dai, 2017; Mintz and Walker, 1993; Nemani et al., 2003; Pan et al., 2015). However, soil moisture changes in response to the Mt. Pinatubo eruption (1991) are underreported in the literature, and it is unclear how soil moisture would respond given volcanically forced changes in primary drivers (temperature and precipitation). Studying a large (10xPinatubo) volcanic eruption, (Frölicher et al., 2011) have shown that the terrestrial carbon pool is sensitive to the regional (in the tropics and sub-tropics) soilmoisture content through the net-ecosystem productivity. Using the geoengineering large

100

101

102

103

104

105

106

107

108

109

110

111

112

113

114

115

116

117

118

119

120

121

ensemble simulations with the CESM model, (Cheng et al., 2019) have analysed the changes in
terrestrial hydrological cycle and discussed the future soil-moisture response and its drivers
under a geoengineering scenario. To our knowledge, no study has yet investigated multiple
indicators of water use with agricultural productivity after a short-duration event like Mt.
Pinatubo eruption. Hence, this study looks to explicitly investigate changes in agricultural
drought indices from Mt. Pinatubo by considering the store (soil moisture) and flux
(evapotranspiration) of water as potential short-term controls over productivity in particular
regions. We use NASA's state-of-the-art Earth system model-with interactive aerosol chemistry
to conduct the simulation experiments consistent with the counterfactual inference of causation
approach for the Mt. Pinatubo eruption. The Mt. Pinatubo effect in the model-simulated climate
is evaluated through the various pathways of climate impacts, from the primary dependent
variables to the higher order responses controlling plant productivity., which incorporates
prognostically evolving aerosols, to conduct simulation experiments following the counterfactual
inference of causation approach for the Mt. Pinatubo eruption. We assess the impact of the Mt.
Pinatubo eruption on the model-simulated climate via multiple pathways, ranging from primary
dependent variables to higher-order responses that influence plant productivity. The use of
prognostic aerosols enhances the simulations by capturing dynamically consistent feedbacks
between the climate response and volcanic aerosols, including aerosol-radiation interactions and
stratosphere-troposphere energy flux exchanges (McGraw and Polvani, 2024). Considering the
complexity of modeling the terrestrial system, vegetation demographics, and physiological
characteristics, we use the soil moisture and evapotranspiration-based agricultural drought
indices SMDI (soil moisture deficit index) and ETDI (evapotranspiration deficit index)
developed by (Narasimhan and Srinivasan, 2005) to account for agricultural productivity. We

evaluate short-term (weekly) and long-term (seasonal) scale changes in SMDI and ETDI relative to statistics over longer modern time-period, for short-term and long-term scale to account for agricultural productivity. By focusing on soil moisture and evapotranspiration metrics, the major water-based drivers of plant productivity are explored to deepen our understanding of the impacts Mt. Pinatubo hadimpacts on plant productivity. 2.0 Method, Experiment, and Data 2.1 NASA GISS ModelE2.1 (MATRIX): We use the state-of-the-art Earth system model from the NASA (National Aeronautics and Space Administration) Goddard Institute for Space Studies, NASA GISS ModelE2.1 (Bauer et al., 2020; Kelley et al., 2020). NASA GISS ModelE2.1 has an atmospheric horizontal latitude-longitude grid spacing of 2.0x2.5 degrees (at the equator) with 40 vertical levels and a model top ofat 0.1 hPa. We used the interactive chemistry version MATRIX (Multiconfiguration Aerosol TRacker of mIXing state) aerosol microphysics module (Bauer et al., 2008, 2020), which is based on the Quadrature Method of Moment (QMOM) to predict aerosol particle number, mass, and size distribution for 16 different mixed modes of the aerosol population. New particle formation is represented by Vehkamäki et al. (2002), along with aerosol-phase chemistry, condensational growth, coagulation, and mixing states (Bauer et al., 2013). 16 mixing states with 51 aerosol tracers for sulfate, nitrate, ammonium, aerosol water, black carbon, organic carbon, sea salt, and mineral dust are resolved in this microphysical module (Bauer et al., 2008, 2020). The first indirect effect of aerosols in terms of changes in cloud properties through nucleation is also computed within MATRIX. The model's ocean component (GISS Ocean v1) of the model has a horizontal resolution of 1x1.25 degrees, with 40 vertical layers. The land component is the Ent Terrestrial Biosphere

146

147

148

149

150

151

152

153

154

155

156

157

158

159

160

161162

163

164

165

166

167

168

169

Model (TBM) (Kim et al., 2015; Kiang 2012) which includes an interactive carbon cycle (Ito et

al., 2020), satellite-derived (MODIS-Moderate Resolution Imaging Spectroradiometer) plant functional type, and monthly variation of leaf area index (Gao et al., 2008; Myneni et al., 2002), and tree height (Simard et al., 2011). Interannual variations in the vegetation properties are controlled by rescaling the vegetation fraction (Figure S6) using historical crops and pasture at grid scale to account for land cover and land use changes (Ito et al., 2020; Miller et al., 2020). Interannual variations in the vegetation properties are controlled by rescaling the vegetation fractions (Figure S8) using historical crops and pasture at the grid scale to account for land cover and land use changes (Ito et al., 2020; Miller et al., 2021). The land model has two defined tiles for the soil layer: bare and vegetated, and each has six vertical levels to a depth of 3.5 m (11.5 feet) (Rosenzweig and Abramopoulos, 1997). Rooting depthdepths for different plant functional typetypes are also given by Rosenzweig and Abramopoulos (1997), and more than 60% of roots for crop plant functional typetypes are located within 0.6 m (1.96 feet) of soil depth. In this version of the model, for the agricultural grid cells, crop plant functional type, and crop calendar are prescribed according to-McDermid et al., (2019). Irrigation in the GISS ModelE is implemented using the water irrigation demand data (IWD₇) (Wisser et al., 2010) and irrigation potential calculations based on (Wada et al., 2013) as discussed in (Cook et al., 2020). 2.2 Experiment Design: The MATRIX version of GISS ModelE2.1 with active tracers is three times more computationally expensive than the non-interactive (prescribed pre-calculated aerosol concentration and extinction) version. We extended an equilibrated 1400-yearlong PI control run with non-interactive tracers with an additional 500 years using the MATRIX version with prognostic tracers before starting the 'historical' run. MATRIX includes the tropospheric chemistry scheme that includes contains the inorganic (Ox NOx Hox and CO), organic chemistry of CH4, and higher hydrocarbons (Gery et al., 1989; Shindell, 2001; Shindell et al., 2003). The

170

171

172

173

174

175

176

177

178

179

180

181

182

183

184

185

186

187

188

189

190

191

stratospheric chemistry includes bromine, chlorine, and polar stratospheric clouds (Shindell et
al., 2006). Dust emission in the model is controlled by the climate variables such as winds and
soil moisture at the spatial and temporal scales (Miller et al., 2006). However, anthropogenic
dust is not included in GISS ModelE2.1. Other anthropogenic emissions, including biomass
burning (pre-1997 from (van Marle et al., 2017) and 1997 onwards from the GFED4s inventory
(van der Werf et al., 2017)), are taken from the Community Emission Data System (CEDS)
inventory (Hoesly et al., 2018). Most importantly, the volcanic SO ₂ forcing for the 'historical'
run (1850-1977) is the daily emission rate from VolcanEESM (Neely and Schmidt 2016 :
https://catalogue.ceda.ac.uk/uuid/a8a7e52b299a46c9b09d8e56b283d385) and satellite
measurement driven SO ₂ inventory (Carn et al., 2017) for 1978 to 2022. The cumulative Mt.
Pinatubo emission is 15194 kt (~15.2 Tg) of SO ₂ injected from 12 th), and satellite measurement
based SO ₂ inventory (Carn et al., 2016) for 1978 to 2014 (extended up to 2021). The cumulative
Mt. Pinatubo emission is 15194 kt (~15.2 Tg) of SO ₂ injected from 13 th to 16 th of June 1991
above the Mt. Pinatubo vent, with a maximum of 15000 kt (15 Tg) emitted on June 15th at a
plume height of 25 km (DiehlCarn et al., 2012(2016). The MATRIX version of the GISS
ModelE2.1 used for all of our simulations predicts the nucleation, evolution, and removal of
sulfate aerosols prognostically.
The model simulations we performed (Table 1) are described here. We started from the 1400-
year-long preindustrial control run from CMIP6 (GISS-CMIP6-PI) with the prescribed average
AOD historical period, which is further extended for 500 years using the GISS ModelE2.1 $-$
MATRIX with prognostic tracers (GISS-PI). Then, the CMIP6 historical run (GISS-HIST-SO2;
1850-2014) started with all forcings as specified by CMIP6 except the daily emission rate of
injection of SO2 (VolcanEESM) (Carn et al. 2016; Neely III and Schmidt 2016) We branched

out the experiment ensemble with Mt. Pinatubo eruption (GISS-PIN-SO2) and the counterfactual ensemble without Mt. Pinatubo (GISS-NOPIN-SO2) from the historical (GISS-HIST-SO2) using perturbed initial conditions (1st Jan 1986) from the year 1986 to 1999. The perturbation to the initial conditions is generated by altering the radiation-related random number generator that deals with fractional cloudiness in the column.

Table 1: Simulation experiment designdetails.

		Time period /run	Ensembles# of	Configuration
EXP Name	Description	length	ensembles	
GISS- CMIP6-PI	Preindustrial	1850 climatology /13001400 years	1	GISS ModelE2.1 — MATRIX with prescribed stratospheric aerosols (average volcanic AOD for historical period, 1850-2014)
GISS-PI	Preindustrial	1850 climatology /500 years	1	Extension to GISS- CMIP6-PI using GISS ModelE2.1— MATRIX with prognostic tracers
GISS-HIST- SO ₂	historical	1850-2014 /165 years	1	GISS ModelE2.1 MATRIX with all forcings as specified by CMIP6 except daily emission rate of injection of SO ₂ (VolcanEESM; Neely & Schmidt 2016; Carn et al., 2017)
GISS-PIN- SO ₂	historical	1986-1999 / 15 years	11*	GISS ModelE2.1 MATRIX Branched out from GISS-HIST- SO2, with all forcings as specified by

Deleted Cells

				CMIP6 except daily emission rate of SO ₂ from a combination of VolcanEESM (Neely & Schmidt 2016) and Carn et al., 2017.
GISS- NOPIN-SO ₂	historical	1986-1999 / 15 years	11*	GISS ModelE2.1 — MATRIX with all forcings as according to CMIP6 with daily emission rate of SO ₂ without Mt. Pinatubo from a combination of VolcanEESM (Neely & Schmidt 2016) and Carn et al., 2017.

*These ensemble members are branched out from the GISS-HIST-SO₂ by perturbing a radiation-related random number generator that deals with fractional cloudiness in the columnthe initial conditions.

2.3 Methods: This study aims to explore investigates the impacts of the Mt. Pinatubo eruption on the major drivers of primary productivity, focusing on soil moisture-related metrics and evapotranspiration. Hereafter, we use the terminology 'PCH' (Mt. Pinatubo and Cerro Hudson) to refer to the 'GISS-PIN-SO2' and 'NP' for the counter-factual ensemble 'GISS-NOPIN-SO2'.

Since We have included the Cerro Hudson eruption in both ensembles since we are focusing on the Mt. Pinatubo—driven climate response, we have included the Cerro Hudson eruption in both ensembles.

2.3.1 Statistical analysis <u>used to detectfor detecting</u> Mt. Pinatubo-significant regions and <u>calculate their</u> anomalies <u>calculations</u>.

We treat the no-Pinatubo ensemble (NP) as a counter-factual climate simulation and utilize it to perform the paired Student's t-test. The null hypothesis is that the ensemble means of a quantity of interest (QoI) in a region over a time period are the same between ensembles: (i.e. $H_0: \bar{\mu}_{PCH} = \bar{\mu}_{NP}$. Regions filled in grey in). In the subsequent figures in this document-, gray regions indicate that non-rejection of the null hypothesis cannot be rejected at the 95% confidence level. Regions in which the null hypothesis is not accepted are highlighted in color in subsequent plots, where, while the color huescolored areas highlight its rejection and show anomalies with respectrelative to the 1950-2014 simulated climatology (see Supplementary information section S1.0). However, directly comparing the difference between the two ensembles (PCH and NP) is an alternative approach to presenting the Pinatubo effect (see Supplement Figure S2). Using either approach leads to the same general conclusions, with only small quantitative differences. Nevertheless, we chose to remain consistent with the baseline requirements for other metrics as well and used the historical climatology for the period 1950-2014. as the baseline for the core of our analysis. The coloring is done to emphasize emphasizes the significant regions of anomalies, but. But we also emphasize the difference in calculations: the grey regions areas show no significant change between the PCH and NP ensembles, while the anomalies are PCH ensemble mean minus climatology. 2.4 Impact metrics The distribution of incoming and outgoing radiation influences the hydrological cycle (Kiehl and Trenberth, 1997; Trenberth and Dai, 2007). A reduction of solar radiation at the surface has the potential to reduce rainfall and change the latent heat-dominated atmospheric heating pattern (Trenberth and Stepaniak, 2004). The perturbed atmospheric conditions and surface energy budget could affect soil moisture. Along with the surface air temperature and precipitation, we

235

236

237

238

239

240

241

242

243

244

245

246

247

248

249

250

251

252

253

254

255

256

use soil moisture and surface energy budget-oriented drought indices (the soil moisture deficit index (SMDI) and evapotranspiration deficit index (ETDI)) to evaluate the land-atmosphere interaction and account for the potential drivers to the crop plant productivity in the model simulated post-Mt. Pinatubo environmental conditions (Narasimhan and Srinivasan 2005). SMDI represents the land-based soil moisture state in selected depth horizons (i.e. of the crop plant productivity in the model simulated post- Mt. Pinatubo environmental conditions (Narasimhan and Srinivasan, 2005). SMDI represents the land-based soil moisture state in selected depth horizons (i.e., SMDI 2 means Soil Moisture Deficit Index for 2 feet (0.6 m) depth). ETDI represents the atmospheric conditions governing the land-atmosphere interaction and is also an indicator of plant health. Lastly, plant transpiration is analyzed to the explore the simulated physiological response to the volcanically induced hydroclimatic conditions. The Palmer drought severity index (PDSI) and other indices are commonly used to represent climatological drought conditions, but. However, we focus on SMDI and ETDI because these can represent capture short-term developing agricultural drought conditions as a response to that impact plant productivity and are free from the limitations of other metrics like PDSI. For example, SMDI and ETDI are seasonally independent measures and are comparable across space, even for different climatic zones.

258

259

260

261

262

263

264

265

266

267

268

269

270

271

272

273

274

275

276

277

278

279

280

SMDI and ETDI were calculated as described in Narasimhan and Srinivasan (2005) using model output at monthly and daily scales. Daily model output is resampled to a weekly scale to compute the indices. Weekly The weekly frequency is used because it is suitable for agricultural applications, and the daily frequency is comparatively higher-and, which makes these indices computationally expensive for such indices. Below, we reproduce the weekly calculation of SMDI and ETDI as presented in Narasimhan and Srinivasan (2005).

281 282

283

284

spanning 1950-2014.

be calculated as

 $SMDI_i = 0.5 * SMDI_{i-1} + SD_i/50$

285

286

And

287

288

289 290

291

292

293

294

295

296 297

298

299 300

302

301

303

2.4.2 Evapotranspiration Deficit Index (ETDI): The limitations of the Palmer Drought

Severity Index (PDSI;) (Palmer, 1965) and Crop Moisture Index (CMI;) (Palmer, 1968)) in the

content between 4 (1.2 m) to 6 feet (1.8 m) in depth.

2.4.1 Soil Moisture Deficit Indices Index (SMDI): Soil The soil moisture deficit index measures

the wetness/dryness of the soil moisture condition conditions in comparison to long-term records

SD_{i,j} is the soil water deficit (%) for week j of the year i. SW_{i,j} is the mean weekly soil water

available in the soil profile (mm) for week j of the year i, MSW_j is the long-term (calibration

the jth weekly minimum and maximum of soil water available in the soil profile across the

..... (2.4.1c)

period) median available water in the soil profile (mm) for week j, and minSWi and maxSWi are

calibration period (1950-2014). The soil mositure deficit index for any given week can

SMDI can be calculated for different soil depths-of soil; we used the 2, 4, and 6-feet depths for

SMDI estimation, approximately 0.6, 1.2, and 1.8 meters, respectively. For SMDI, it is typical to

use feet instead of meters in the literature, which is why we use the same units here:along with

between 2 (0.6 m) to 4 feet (1.2 m) in depth. Similarly, SMDI-6 indicates the soil moisture

the coventional SI units in brackets here. SMDI-4 means we considered the soil moisture content

14

 $SD_{i,j} = \frac{sW_{i,j} - MsW_j}{MSW_i - minSW_i} \times 100 \ \ if \ SW_{i,j} \ \leq \ MSW_j \qquad \ldots \ldots (2.4.1a)$

 $SD_{i,j} = \frac{sw_{i,j} - MsW_j}{maxSW_j - MsW_j} \times 100 \ \ if \ SW_{i,j} > MSW_j \qquad \ldots \ldots \ (2.4.1b)$

formulation used for PET calculation (Thornthwaite, (1948) calculation and lack of accountability to the land cover type on water balance encouraged the exploration of ETDI for agricultural productivity. Also, in the climate models, surface energy fluxes are parameterized in terms of the thermodynamicalthermodynamic gradient of atmosphere and land models and thus represent the land-atmosphere interactions, which are not accounted for by these atmosphereonly indices. We utilized model simulated surface energy fluxes (Latent and Sensible heat) to calculate the potential (PET) and actual evapotranspiration (AET) to estimate the water stress ratio. However, the applicability of the Penman-Monteith equation for reference crops (Allen et al., (1998) provides a substitute method for PET calculation, which, although not shown, broadly produced similar results-(not shown). In Equation Equations 2.4.2a and 2.4.2b-, we used the model simulated energy fluxes to calculate AET and PET as suggested in (Milly and Dunne, 2016; Scheff and Frierson, 2015). The energy budget equation at the surface is given by Rn= G + LH+SH, where Rn is incomingnet solar radiation, G is net ground energy, heating (heat flux), LH and SH represent the Latent and Sensible heat fluxes, respectively. We then use these to calculate PET and AET (unit as mm per day):; $1 \text{ Wm}^{-2} = 0.0353 \text{ mm/day}$: $PET = 0.8(R_n - G) = (0.8 * 0.0864/2.450353) * (LH + SH) (2.4.2a)$ And AET = LH* (0.0864/2.450353)...... (2.4.2b) The evapotranspiration deficit index is estimated using the water stress condition using the actual evapotranspiration (AET) and potential evapotranspiration (PET) per grid cell, as given below. $WS = \frac{PET - AET}{PET}$ (2.4.2c)

304

305

306

307

308

309

310

311

312

313

314

315

316

317

318 B19

320

321

322

323

324

WS ranges between range, from 0 to 1, where 0 signifies that evapotranspiration is happening at

327 the potential rate and 1 standsstand for no actual evapotranspiration. WS represents the water

stress ratio aton a monthly or weekly basis (WS_j), which is further utilized to calculate water

329 stress anomaly (WSA_{i,j}) for week j of year i as given below.

B30 WSA_{i,j} =
$$\frac{MWS_j - WS_{i,j}}{MWS_i - minWS_i} \times 100$$
 if WS_{i,j} $\leq MWS_j$ (2.4.2d)

331 And

334

335

340

341

342

344

345

346

347

348

332
$$WSA_{i,j} = \frac{MWS_j - WS_{i,j}}{maxWS_j - MWS_j} \times 100 \text{ if } WS_{i,j} > MWS_j \dots (2.4.2e)$$

Here, MWS_i, minWS_i, and maxWS_i represent the longtermlong-term median, minimum, and

maximum of the water stress ratio over the calibration period. Water stress anomaly ranges

between -100% to 100%, indicating very dry to wet conditions over the region.

Finally the severity of the, drought conditions everity is calculated as ETDI, similar to SMDI

337 (equation 2.4.1c) at a monthly/weekly time scale.

338 ETDI_j =
$$0.5 * ETDI_{j-1} + WSA_j / 50$$
. (2.4.2f)

339 The indices SMDI and ETDI range from -4 to +4, representing the excessive wet and dry

conditions. The bounding values -4 or +4 represent extremely dry/wet conditions as the

deficit/excess of soil-moisture deficit (SM) or water stress anomaly (WSA) is-reached, relative to

the maximum over the reference calibration period.

We also highlight the justification for selecting 1950-2014 as the base period for

analyzing the response in climate variables and the long-term calibration period for drought

indices calculations. (Supplementary information section <u>4sS1</u>).

3.0 Results

The result section of this study first presents the NASA GISS model's simulated

properties of the 1991 Mt. Pinatubo eruption, and then further evaluates the evaluation of the

primary (aerosol optical depth, radiation, and temperature) and secondary (precipitation, soil moisture, evapotranspiration, and transpiration) impacts on plant productivity.

3.1 Radiative forcings and forcing response

349

350

351

352

353

354

355

356

357

358

359

360

361

362

363

364

365

366

367

368

369

370

371

We analyze the microphysical and radiative properties of volcanic aerosol simulated by the NASA GISS ModelE (MATRIX) in the PCH ensemble set. The current setup of GISS ModelE uses the aerosol microphysical module MATRIX represent the various states and provide particle number, mass, and size information for different mixed modes of the aerosol population. In the simulation of the Mt. Pinatubo eruption In the Mt. Pinatubo eruption simulation, the volcanically injected SO₂ in the stratosphere oxidizes in the presence of prognostically evolving OH radicals to form the stratospheric sulfate aerosols. Sulfate aerosols grow by condensation of gas (nucleation, and self-coagulation (preexisting)) to the Aitken (AKK) mode (mean mass diameter <0.1 μm), and further growth in size leads to the transfer to Accumulation (ACC) mode (Bauer et al., 2008; Bekki, 1995). The transfer between the two particle modes is controlled through the transfer function based on particle mean mass diameter (Bauer et al., 2008). GISS ModelE (MATRIX) PCH simulated a sulfate aerosol size with an effective radius (R_{eff}) of the order of 0.3-0.6 μ m after the Mt. Pinatubo eruption (not shown), eonsistent with several observation and modeling estimates (Bauman et al., 2003; Bingen et al., 2004; Russell et al., 1996; Stenchikov et al., 1998). GISS ModelE (MATRIX) PCH simulated a peak global mean aerosol optical depth (AOD; for 550 nm wavelength) of 0.21 (Supplementary Fig S2 bottom panel) a few months after the eruption, which then decreases due to deposition (Supplementary section S2.0). GISS ModelE (MATRIX) PCH also simulated a peak global mean aerosol optical depth (AOD; for 550 nm wavelength) of 0.22 (Supplementary Fig S4 bottom panel) a few months after the eruption, which then decreases with time due to the deposition of

<u>volcanic aerosols</u> (English et al., 2013; Sato et al., 1993). <u>HereIn this study</u>, the model-simulated <u>extinction of the radiationaerosol optical depth</u> (AOD) due to volcanic aerosol and radiative forcing is larger than <u>the previously reported AOD of 0.15</u> and forcing of _-4.0 to -5.0 Wm⁻² due to the Mt. Pinatubo eruption (Hansen et al., 1992; Lacis et al., 1992).

372

373

374

375

376

377

378

379

380

381

382

383

384

385

386

387

388

389

390

391

The mass and size of volcanic sulfate aerosol firmly control the scattering of the incoming shortwave radiation and the absorption of longwave (Brown et al., 2024; Kinne et al., 1992; Lacis, 2015; Lacis et al., 1992; Lacis and Hansen, 1974)(Kinne et al., 1992; Lacis, 2015; Lacis et al., 1992; Lacis and Hansen, 1974). The first-order climate response to the volcanicallyinjected sulfate aerosol in the stratosphere is the perturbation of the radiative balance of the Earth system (Hansen et al., 1980; Lacis et al., 1992; Stenchikov et al., 1998). Figure 1The first-order climate response to the volcanically-injected sulfate aerosol in the stratosphere is the perturbation of the radiative balance of the Earth system (Brown et al., 2024; Hansen et al., 1980; Lacis et al., 1992; Stenchikov et al., 1998). Supplementary figure S3 shows that the GISS ModelE PCH has simulated a peak longwave, shortwave, and net radiative response of +3.0 Wm⁻², -8.0 Wm⁻², and -5.0 Wm⁻² respectively, a few months after the eruption, which recovers slowly in next 24 months and is consistent with previous studies (Stenchikov et al., 1998; Hansen et al., 1992; Minnis et al., 1993; Brown et al, 2024). These radiative responses are calculated with respect to the climatology for the period 1950-2014 in GISS-Hist-SO2. The GISS model also simulated a smaller peak ranging within -1 Wm⁻² in the counterfactual (without Mt. Pinatubo) runs, likely due to the Cerro Hudson eruption in August 1991.

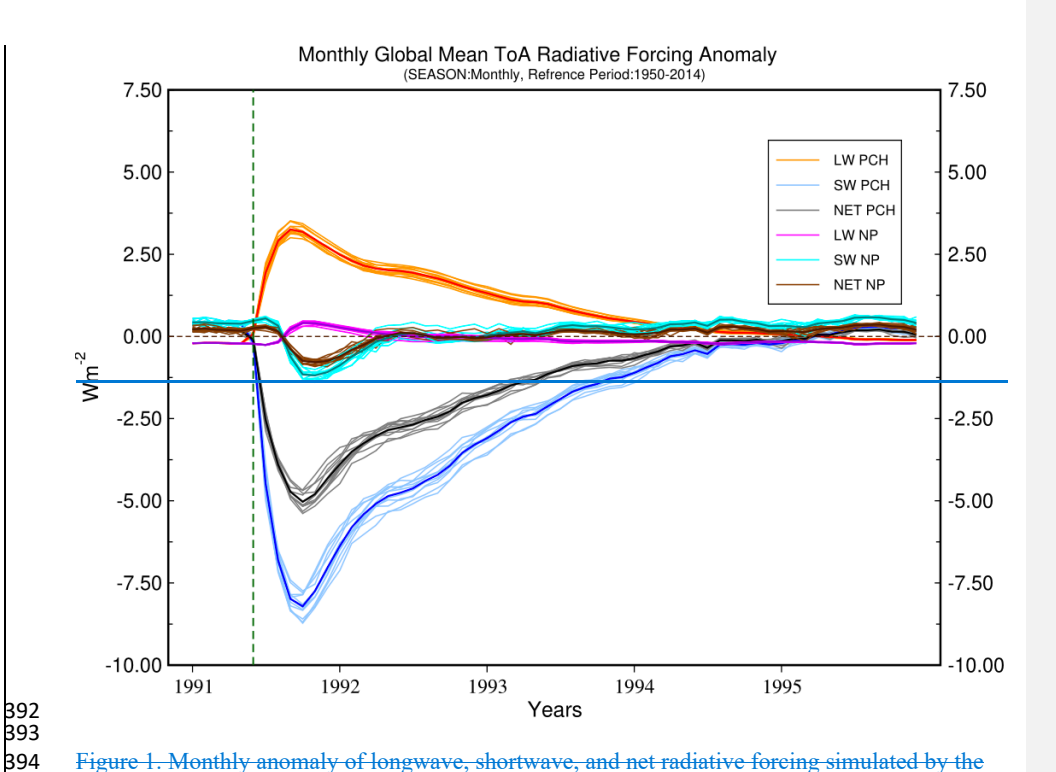
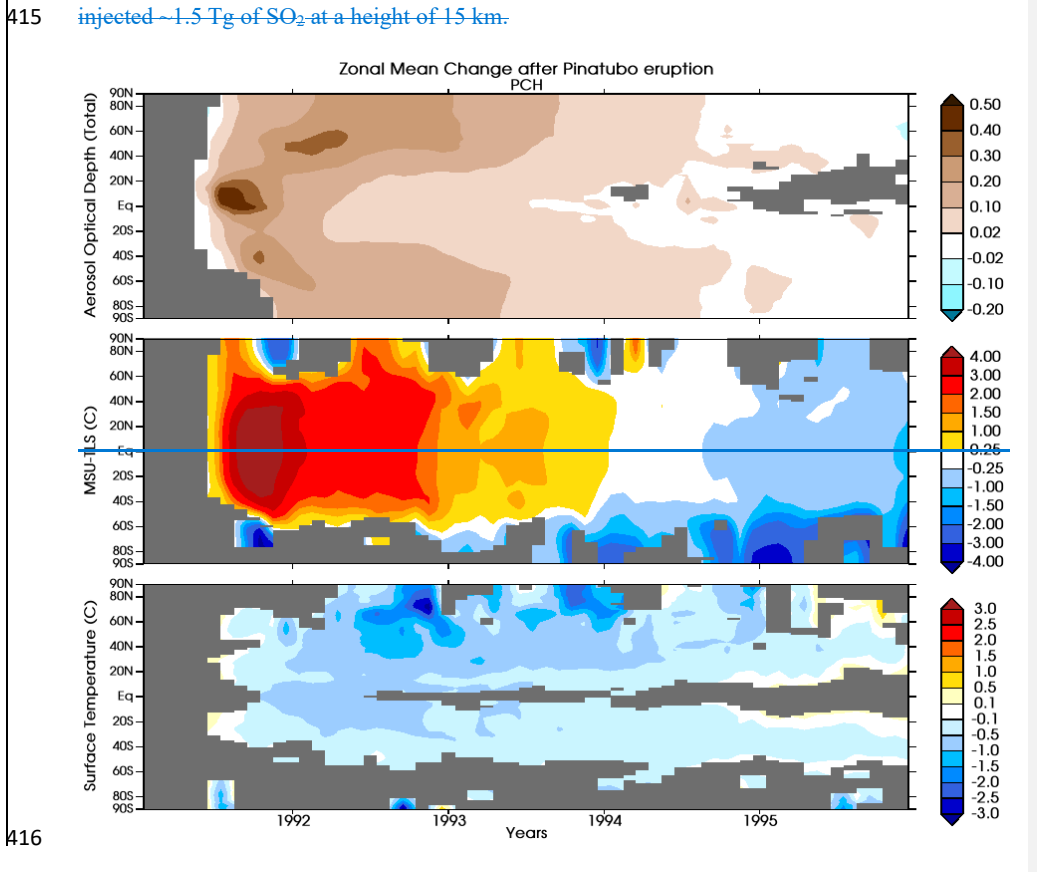


Figure 1. Monthly anomaly of longwave, shortwave, and net radiative forcing simulated by the GISS ModelE for Mt. Pinatubo (PCH) and counterfactual (NP) ensemble. The response anomalies are calculated with respect the climatology for the period 1950-2014, taken from the GISS historical runs (GISS-HIST-SO2). The light-colored thin lines represent the individual ensemble member, and the dark broad line is multi-ensemble mean for each variable (longwave, shortwave and net radiative response).

3.2 Aerosol dispersion and Temperature Response temperature response

Figure 2 shows the zonal mean anomaly for the aerosol optical depth (AOD), lower stratosphere temperature (MSU-TLS satellite simulator), and surface temperature. The zonal AOD shows the dispersion and transport of aerosol poleward after the eruption. Horizontal dispersion and transport of the aerosols is strictly influenced by the stratospheric meteorology and atmospheric circulation, which is independent in each ensemble member, and depends on the

plume height and season. GISS ModelE has simulated AOD consistently with previous studies (Aquila et al., 2012; Brown et al., 2024; Rogers et al., 1998; Timmreck et al., 1999; Trepte et al., 1993). Cross-equatorial dispersion to the southern hemisphere might be due to the more robust Brewer-Dobson circulation in the austral winter (Aquila et al., 2012). Meanwhile, the phases of QBO and local heating also play a crucial role in the poleward and vertical dispersion of stratospheric aerosols (Hitchman et al., 1994; Ehrmann et al., 2024 (in-prep)). A smaller peak in the southern hemisphere (45° S) in later 1991 likely due to the Cerro Hudson cruption, which injected ~1.5 Tg of SO₂ at a height of 15 km.



depth at 550 nm (top panel), microwave sounding unit temperature (MSU-TLS) for lower stratosphere (middle panel) and surface air temperature with respect to the 1950-2014 climatology. Gray regions show no statistically significant difference between the PCH and NP responseFigure 1 shows the zonal mean anomaly for the aerosol optical depth (AOD) and surface air temperature. The zonal AOD shows the dispersion and transport of aerosol poleward after the eruption. Horizontal dispersion and transport of the aerosols are strictly influenced by the stratospheric meteorology and atmospheric circulation, which is independent in each ensemble member, and depends on the plume height and season. GISS ModelE has simulated AOD consistently with previous studies (Aquila et al., 2012; Rogers et al., 1998; Timmreck et al., 1999; Trepte et al., 1993). Cross-equatorial dispersion to the southern hemisphere might be due to the more robust Brewer-Dobson circulation in the austral winter (Aquila et al., 2012). Meanwhile, the phases of QBO and local heating also play a crucial role in the poleward and vertical dispersion of stratospheric aerosols (Hitchman et al., 1994). A smaller peak in the southern hemisphere (45° S) in the late 1991, likely due to the Cerro Hudson eruption, which injected ~1.5 Tg of SO₂ at a height of 15 km. The lower panels in Figure 1 show the surface air. The colored areas show anomalies of PCH with respect to the climatology from 1950-2014. The middle and lower panels in Figure 2 show the model-simulated microwave sounding unit (MSU) temperature for the tropical lower stratosphere (TLS) response due to absorption of longwave radiation and for the surface temperature response due to the net radiative perturbation, which is dominated by the scattering of incoming solar radiation. The model simulates a peak

Figure 2. Zonal mean of monthly anomalies for multi ensemble mean for aerosol optical

417

418

419

420

421

422

423

424

425

426

427

428

429

430

431

432

433 434

435

436

437

438

439

440

warming of over 4 °C in the tropical lower stratosphere shortly after the eruption, which lasts for

a few months when the concentration of sulfate aerosols is highest. Significant warming in the range 2-3 °C lasts until the end of 1992, and overall simulated stratospheric warming is consistent with previous studies. Figure S2 (top panel) shows a steplike transition with time with a global mean increase of 3.0 °C in the lower stratosphere temperature after the Mt. Pinatubo eruption followed by a trend consistent with Ramaswamy et al., (2006). The zonal structure of surface temperature shows that the surface cooling follows the aerosol optical depth pattern, and the greatestmost significant cooling is simulated in the northern hemisphere high latitudes. Temporal characteristics of lower stratosphere warming, and surface cooling also show the seasonal variations in incoming solar radiation in northern polar latitudes. Model simulated the lower stratospheric warming due to longwave radiation absorption in lower stratosphere consistent with previous studies (Supplementary text section S3.0).

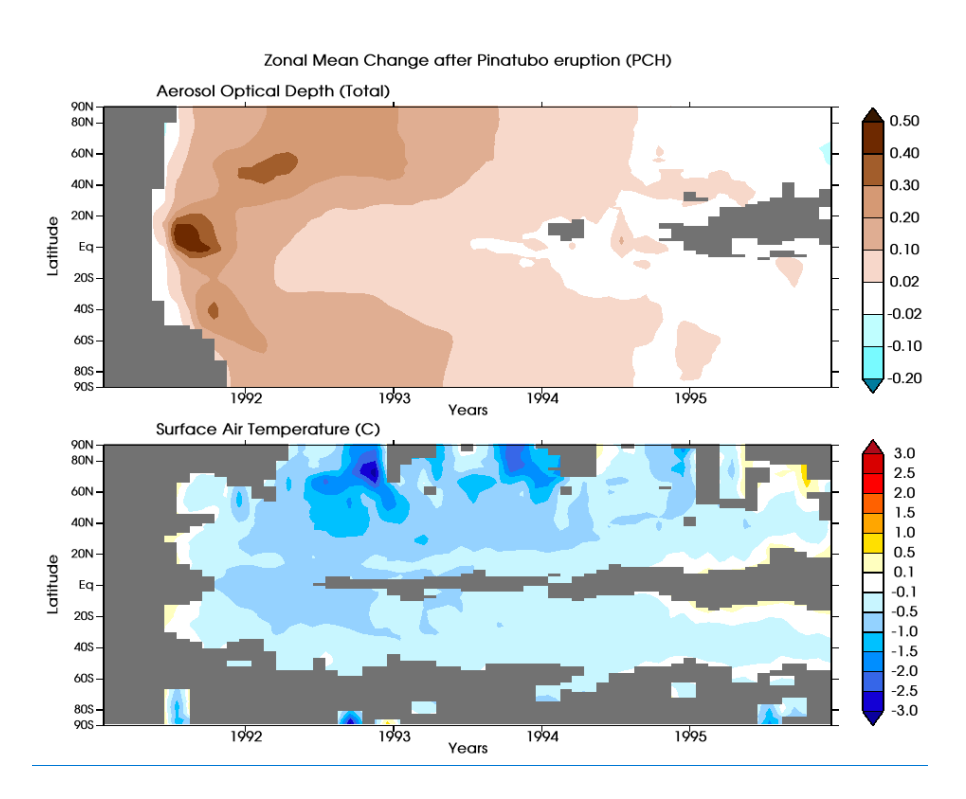


Figure 1. Zonal mean of monthly anomalies for multi-ensemble means for aerosol optical depth at 550 nm (upper panel) and surface air temperature (lower panel) with respect to the 1950-2014 climatology. Gray regions show no statistically significant difference between the PCH and NP responses. The colored areas show anomalies of PCH with respect to the climatology from 1950-2014. of sunlight in northern polar latitudes.

The spatial pattern of surface air temperature response is evaluated at the seasonal scale for each year from 1991 to 1995 as shown in Figure 3. We conclude that the volcanic forcing from the Mt. Pinatubo eruption results in a statistically different seasonal mean surface air temperature response. Figure 3 shows that a spatial pattern of surface cooling starts appearing after a few months of the eruption (during the SON season of the year 1991) when the gaseous

SO2 is oxidized into sulfate aerosols. The surface cooling signature due to the volcanic aerosols is significant in 1992 and 1993 before recovering in 1994 towards pre-eruption temperature conditions. The highest surface cooling is noticed over the sub-tropics and higher latitude land regions in the northern hemisphere and reaches up to 2.5 °C at a regional scale., as shown in Figure 2. We conclude that the volcanic forcing from the Mt. Pinatubo eruption results in a detectable seasonal mean surface air temperature response. Figure 2 shows that a spatial pattern of surface cooling starts appearing after a few months of the eruption (during the SON season of 1991) when the gaseous SO₂ is oxidized into sulfate aerosols. The surface cooling signature due to the volcanic aerosols was significant in 1992 and 1993 before recovering in 1994 towards preeruption temperature conditions. The highest surface cooling is noticed over the sub-tropics and higher latitude land regions in the northern hemisphere and reaches up to 2.5 °C at a regional scale. To summarize: the PCH GISS ModelE simulated global mean peak cooling response is ~0.5 °C after the eruption, as shown in Supplement Figure S4 (Middle panel), with a range between 0.25 – 1.0 °C for individual ensemble members, and this is consistent with the various observation and modeling studies (Dutton and Christy, 1992; Hansen et al., 1996; Kirchner et al., 1999; Minnis et al., 1993; Parker et al., 1996; Ramachandran et al., 2000; Stenchikov et al., 1998). To summarize: the PCH GISS ModelE simulated global mean peak cooling response is ~0.5 °C after the eruption as shown in Supplement figure S2 (Middle panel) with a range between 0.25 - 1.0 °C for individual ensemble members, and this is consistent with the various observation and modeling studies (Brown et al., 2024; Dutton and Christy, 1992; Hansen et al., 1996; Minnis et al., 1993; Parker et al., 1996; Ramachandran et al., 2000; Stenchikov et al., 1998)(Kirchner et al., 1999).

465

466

467

468

469

470

471

472

473

474

475

476

477

478

479

480

481

482

483

484

485

486

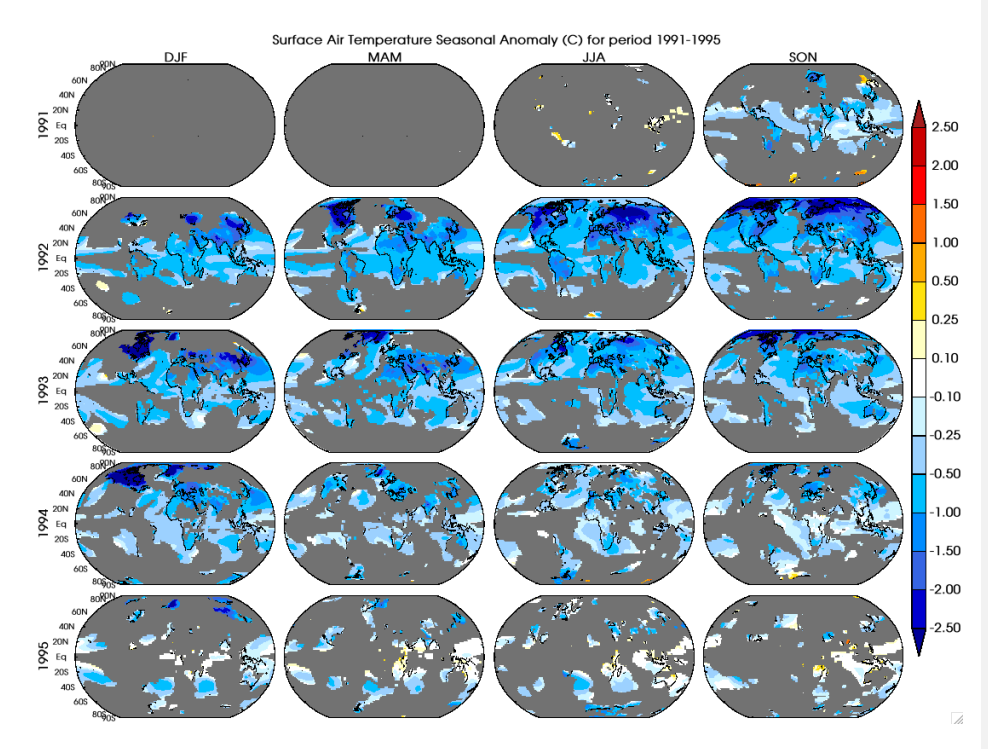


Figure 32: Seasonal mean surface temperature anomalies (°C) from the year 1991 to 1995 with respect to the reference period of 1950-2014. A grey color is painted over the grid cells where the surface temperature anomalies are not statistically significant in comparison to the counterfactual ensemble. The colored areas show anomalies of PCH with respect to the climatology from 1950-2014.

3.3 Rainfall Response

Precipitation, presented seasonally for the year of eruption (1991) and the following year (1992) in Figure 43, shows a highly complex and variable response to the volcanically induced tropospheric cooling and radiative balance perturbation because of its sensitivity to the other climate system components. Studies have shown that global mean precipitation decreases after

large volcanic eruptions (Gu et al., 2007; Gu and Adler, 2012; Iles et al., 2013; Robock and Liu, 1994; Singh et al., 2023; Trenberth and Dai, 2007). Colose et al., (2016) have postulated that the asymmetrical surface cooling and radiative balance perturbation create an energetic deficit in the hemisphere of eruption that constrains the poleward propagation of tropical rainfall belt (ITCZ) in that hemisphere. In the case of the Mt. Pinatubo eruption, the PCH simulations show that regional patches of significant decrease of up to 1 mm per day are spottednoticed over tropical and northern hemispheres (Africa, eastern and northern Asia) after the eruption (Figure 43). Also, increasing rainfall patterns are simulated over the Mediterranean and European regions. Broadly, the confidence level of precipitation response due to volcanic aerosols is strongly influenced by the uncertainty due to many possible factors and prominent modes of atmospheric variability, such as the strength of El Nino (Paik et al., 2020).

The zonal mean of the rainfall response (Figure \$3\subseteq 5) shows a clear decreasing trend in the northern hemisphere tropical and higher latitudes with a positive rainfall response band around 20° N. The PCH modelled rainfall response due to the Mt. Pinatubo eruption is broadly consistent with the previous studies (Joseph and Zeng, 2011; Liu et al., 2016; Trenberth and Dai, 2007), but the uncertainty in rainfall response is still high. Although we use statistical significance at 95% confidence level as our metric offor determining significant anomalies, we do not deny erroneous and only a few regions exhibit a spatially coherent and detectable forced response (Figure 3). We acknowledge the signals due to the model's internal variability when averaging the impacts across multiple ensembles (Polvani et al., 2019). The inconsistency and complexity in the precipitation response drives us to explore the compound hydroclimatic pathways of impacts beyond the rainfall such as droughts, but 11 ensembles are a good compromise between few vs. many ensemble members which was shown to be sufficient to

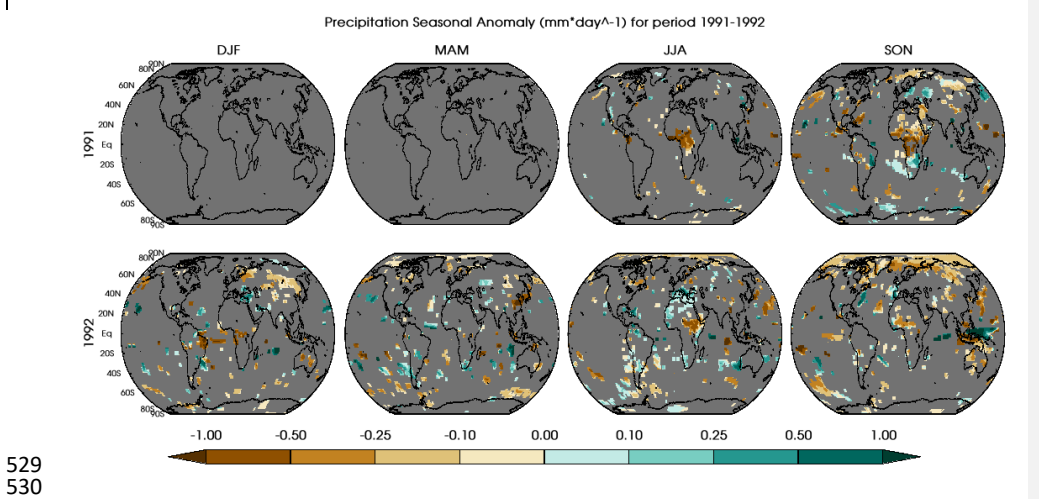


Figure 43. Seasonal mean precipitation anomalies (mm per day) from the year 1991 and 1992 with respect to the reference period of 1950-2014. A grey color is painted over the grid cells where the precipitation anomalies are not statistically significant in comparison to the counterfactual ensemble. The colored areas show anomalies of PCH with respect to the climatology from 1950-2014.

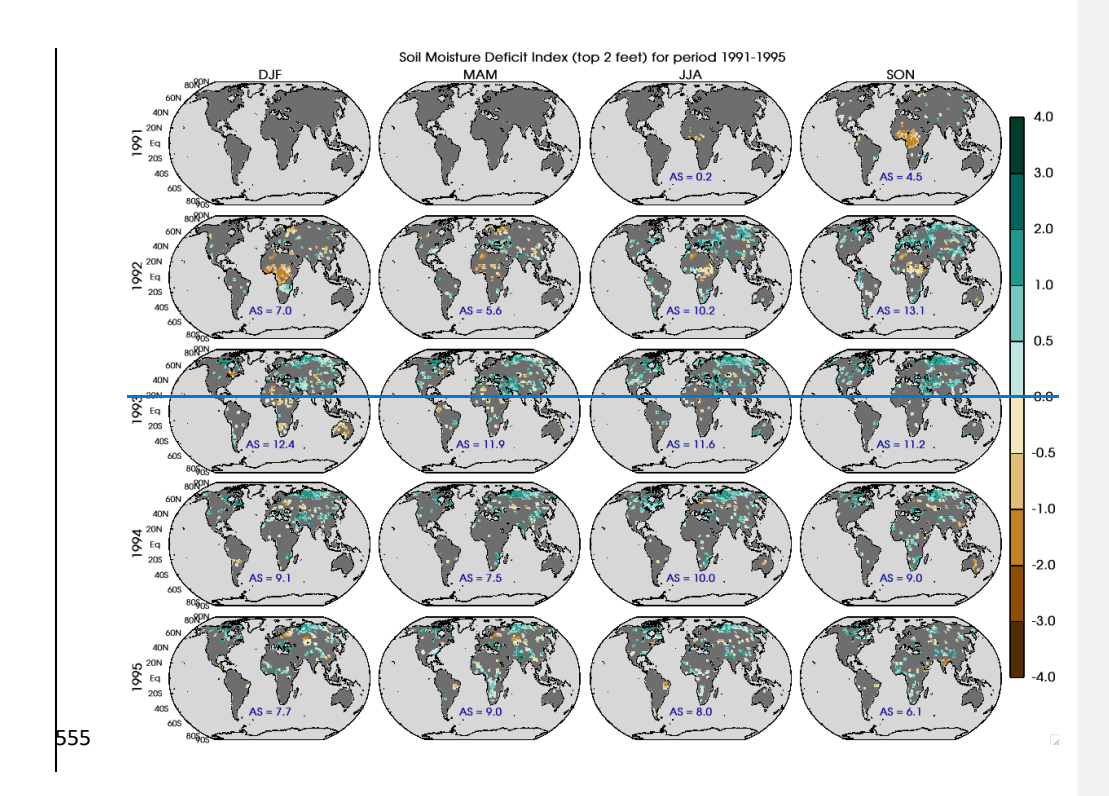
3.4 Drought Conditions

Land-atmosphere interactioninteractions under a radiatively perturbed environment plays are crucial role in regulating the climate response at regional and sub-regional scales. Changes in land-atmosphere interactions on On short timescales, changes in these interactions can strongly affect plant productivity.— Even short-lived adverse conditions in the growth cycle have the potential for outsized impacts, especially if they happen at a particular time in the growing cycle.

Hence, we explore the weekly aspects of these drought conditions in Section 43.6 to explore the temporal characteristics of variability in the conditions.

3.4.1 Seasonal Soil Moisture Drought Index (SMDI)

The root zone is commonly defined as the top 3 – 6 feet (0.9-1.8 m) of the soil column (Keshavarz et al., 2014, and references therein)(Keshavarz et al., 2014) but most agricultural crops have shallower root systems confined to the top 2 feet (0.6 m) (Narasimhan and Srinivasan 2005). Hence, we focus on the soil moisture deficit index (SMDI) (Narasimhan and Srinivasan 2005) for the top 2 feet (0.6 m) of ground depth (SMDI_2) as shown in Figure 54. As anticipated, more land area is covered by statistically different SMDI_2 thenthan in Figure 4 helping to further3. This enhances our analysis of water-driven impact to impacts on plant productivity more then with, offering greater insights than precipitation.



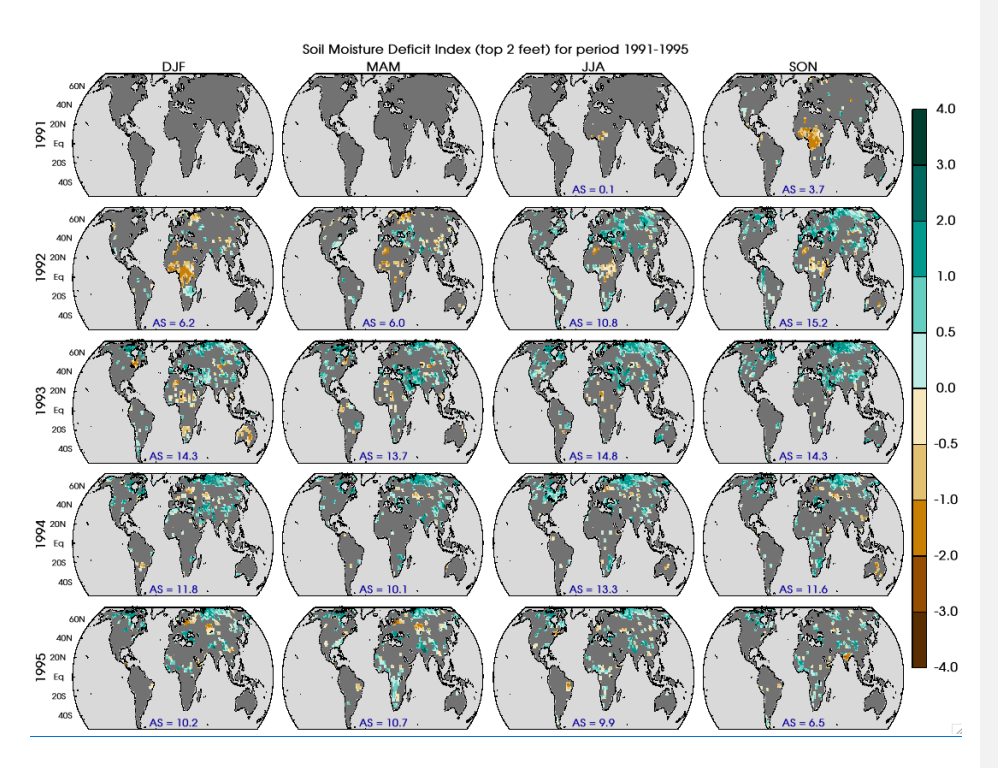


Figure 54. Soil moisture deficit index (SMDI_2) for the top 2 feet(0.6 m) of ground depth evaluated seasonally from 1991 to 1995. Grey color is painted over the grid cell where the SMDI_2 is not statistically significant in contrast to counter-factual ensemble. The parameter AS on each panel markmarks the percentage of land area whichthat has shown statistically significant dry or wet response after Mt. Pinatubo eruption.

Figure 54 clearly shows that the equatorial region, especially over Africa, has a significant drying response due to Mt. Pinatubo in comparisoncompared to long_term historical data-starting from the SON season of 1991 through the following DJF season. Although less robust, the dryness in this region lasted through MAM of 1993. Severity The severity of drying response reaches up to -2.0 on a scale of extreme wet/dry at 4.0/-4.0, where athe severity of – 4.0 reflects the maximum dryness (rarest case) over the entire 1950-2014 calibration period. Figure 43 shows a similar pattern in equatorial African rainfall decrease. Decrease A decrease in rainfall

was present <u>in</u> the first season post_Mt. Pinatubo eruption, indicating an expected lagged response in SMDI_2.- Spatial coherence between these signals is again re-established in the JJA and SON 1992 seasons, albeit with more variation in the strength of the signal.

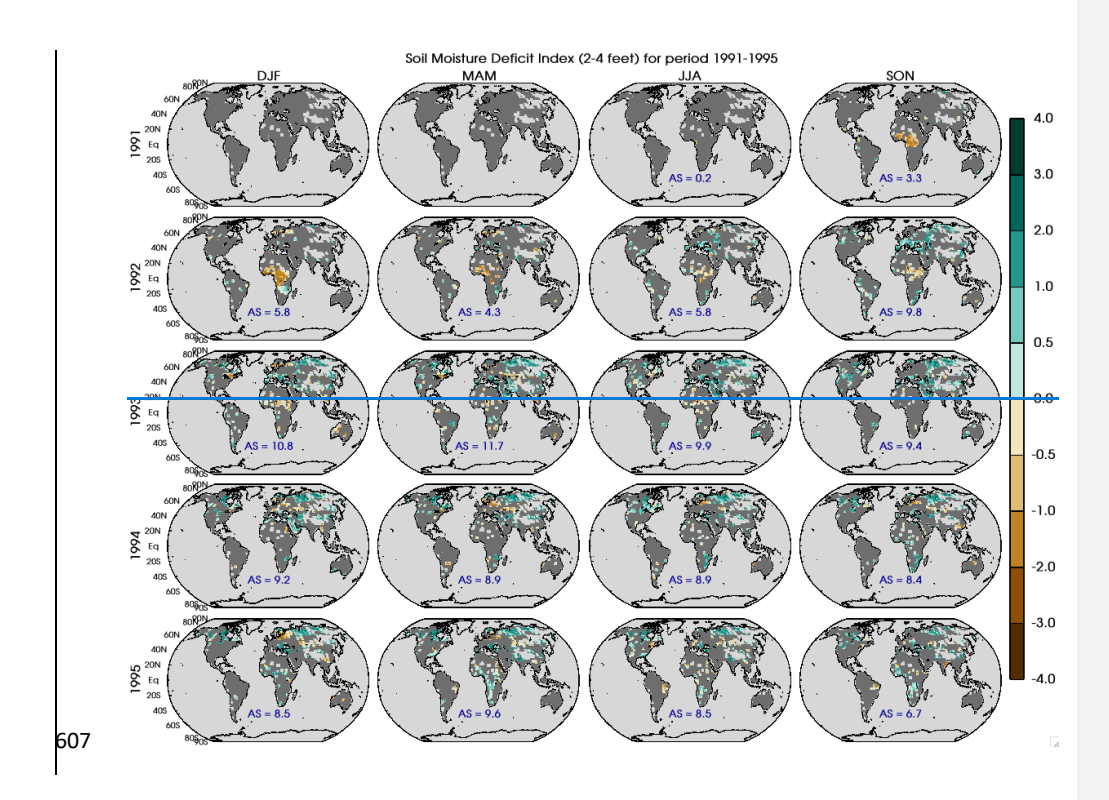
Meanwhile, in the high latitudes of the northern hemisphere, we see an increase in the store of soil moisture despite a decrease in rainfall in higher latitudes.—An exception to this is the Mediterranean (extending towards the east Mediterranean and western AsianAsia) region, where soil moisture and rainfall, both show an increase during post-after the Mt. Pinatubo perioderuption. This increase in the soil moisture in the northern hemisphere is comparatively more pronounced in the summer months than in comparison to the winter seasonsseason. Thus, despite less water supply through rainfall, there ishas been a persistent increase in the soilmoisture in the root zone layer starting fromsince the JJA season of 1992. This is likely due to less water extracted from this layer through evaporation and transpiration as well as due to the implemented irrigation in GISS modelE (details in further sections).

Overall, Figure 54 shows equatorial drying signals mostly dominated through the DJF season of the year 1993, but the wet conditions over higher latitudes lasted till 1995. Broadly, 6-13% of the land region has shown a statistically significance response in terms of dry/wet condition by the end of year 1995 because of the Mt. Pinatubo forcing.

Deeper soil layers <u>better</u> approximate longer-term meteorologically defined drought indices <u>better</u> (Narasimhan and Srinivasan 2005).- This makes intuitive sense:- precipitation provides the recharge for the store of soil moisture, and if there is a longer-term decline in precipitation, all <u>hydraulically</u> available moisture will be used <u>hydraulically</u> for plant transpiration (both the deeper stores of water and the soil-penetrating precipitation available)), not allowing for deeper depth recharge.- Here, we evaluate discrete layer depths instead of

cumulative depths for two reasons.—First, the soil permeability changes with the depth, and the inclusion of top layers erroneously reflects the SMDI_2 signal in potentially impermeable regions; second, the SMDI_2 signal gets superposed over the deeper layer response and misleads the actual soil moisture response for the deeper layers.

As expected, when we evaluate the soil moisture deficit response between 2-4 feet (0.6-1.2 m) soil depth (SMDI_4) in Figure 6.5 and 4-6-feet (1.2-1.8 m) soil depth (SMDI_6) in Figure S4S6, we see similar spatial and temporal distributions as shown in Figure 54 with a corresponding decrease in the percentage of area response.— Spatially, we see high latitudes across North America and Northeastern and western Asia, equatorial Africa, EuropeanEurope, and Mediterranean regions maintain their SMDI-2 trend in Figure 54. However, the total area of response area decreases from peak coverages of 12-13% in SMDI-2 to less than 10-12% in SMDI-4 and 7-10% in SMDI_6 (as shown in Figure S4S6). Additional decreases in the degree of impacts impact are also seen between the three soil layers. Note that the light grey colored regions in Figures 65 and S4S6 represent regions of impermeability, which does affect the total area of response.



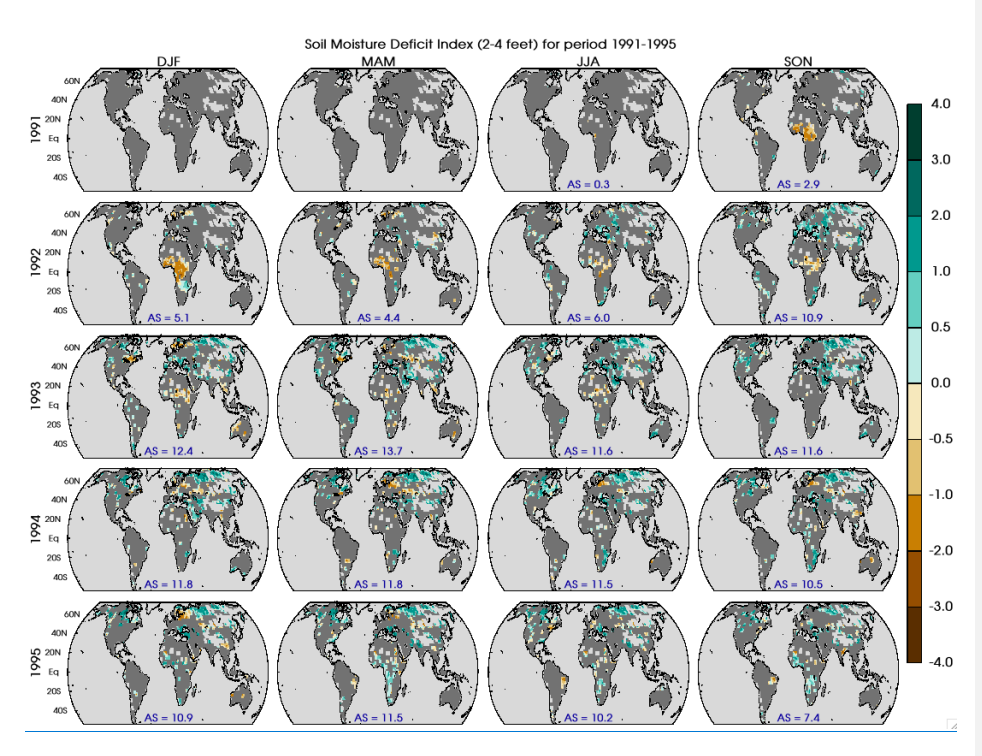


Figure 65. Soil moisture deficit index (SMDI_4) for soil depths between 2-4 feet (0.6-1.2 meter) evaluated seasonally from 1991 to 1995. GreyThe grey color is painted over the grid cell where the SMDI_4 is not statistically significant in contrast to counter-factualthe counterfactual ensemble. The light grey colored regions represent regions of impermeability. The parameter AS on each panel markmarks the percentage of land area which has shownshowing statistically significant dry or wet response after the Mt. Pinatubo eruption.

3.4.2 Seasonal Evapotranspiration Deficit Index (ETDI)

As indicated in the methodology section, ETDI calculation is similar to SMDI but is based on the water stress anomaly, which accounts for the difference between actual and potential evapotranspiration. This ETDI is a measure of the flux of water between land and

atmosphere, and like SMDI_2 in Figure 65, it shows robust statistical differenced over land.

620

621

622

623

624

625

626

627

628

629

630

631

632

633

634

635

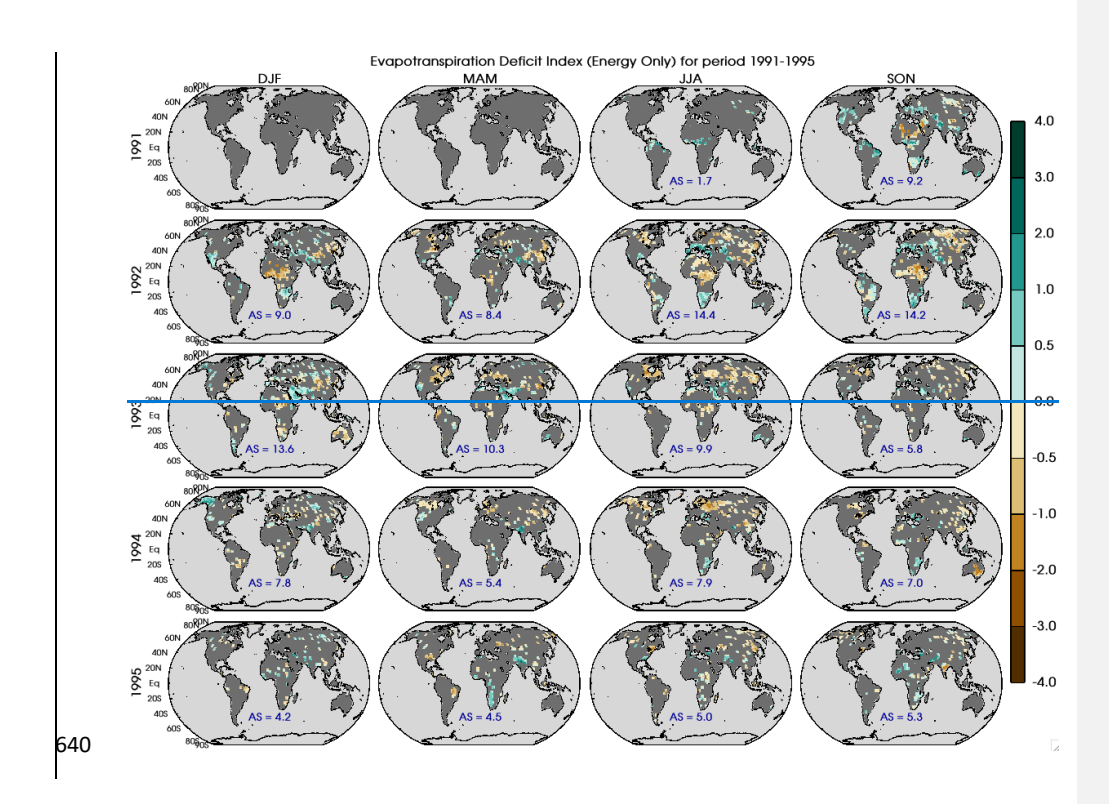
636

637

638

639

Figure 7 shows that 6 illustrates the reduction in ETDI response in the equatorial decreases in ETDI region started developing induring the DJF season forof the year 1992, and these conditions were persistent persisted over the year. Similar to Like SMDI 2, ETDI increases over the regionregions encompassing the Mediterranean and western Asia. However, ETDI differs from the SMDI 2 over some of the northern hemisphere regions, especially-over Northeastern Asia. A drying response in terms of ETDI in the northern hemisphere regions persisted during 1993 and 1994, whereas SMDI 2 shows an opposite response. This contrasting response in terms of through the ETDI and SMDI_2 points to the complexity of land-atmosphere interactions over these regions.- We utilized model simulated surface energy fluxes (Latent and Sensible heat) to calculate the potential (PET) and actual evapotranspiration (AET) to estimate the water stress ratio. In these regions where, soil moisture is available induring the summer and early winter months, but a deficit in. Still, an evapotranspiration deficit reflects the decrease in plant transpiration (latent heat flux), which may be due to the unavailability of plants. Also, the surface temperature (sensible heat flux) response supports the non-water-stressed atmospheric conditions, and thus, overall, it show a deficit inshows an evapotranspiration deficit. Areas of significant response in terms of ETDI varies vary from 7 to 14.5% on a seasonal basis during the years following the eruption. The largestmost significant areas of ETDI coverage occur during the same time periods as SMDI 2 (between JJA 1992 – JJA 1993).



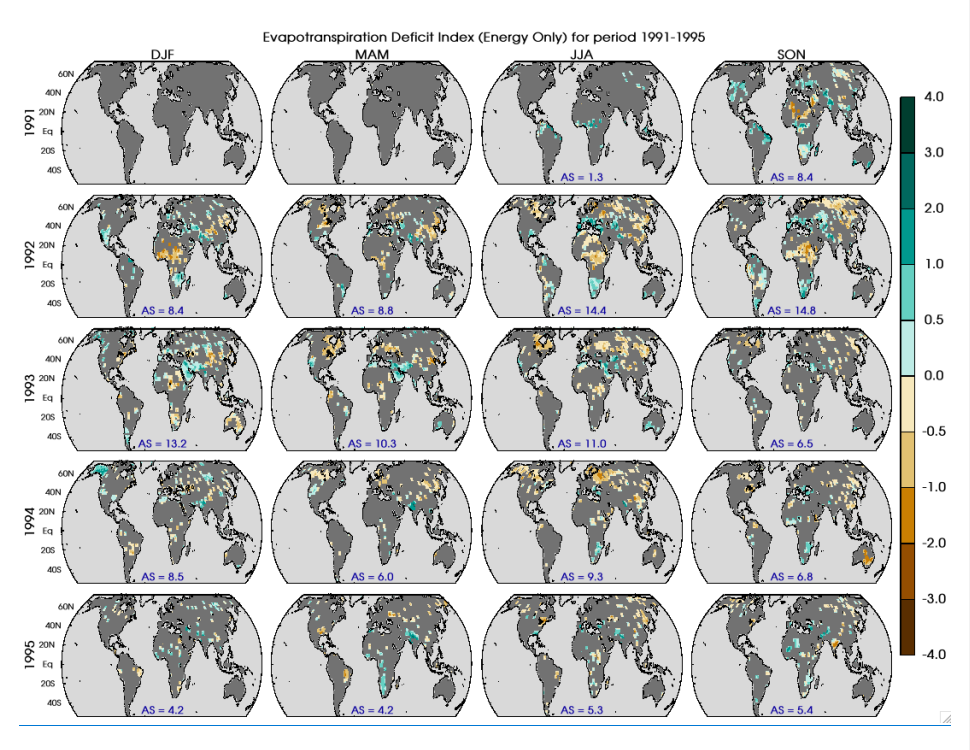


Figure 76. Evapotranspiration deficit index (ETDI) at seasonal scale from 1991 to 1995.

GreyThe grey color is painted over the grid cell where the ETDI is not statistically significant in contrastcompared to counter-factual ensemble. The parameter AS on each panel markmarks the percentage of land area whichthat has shown statistically significancesignificant dry or wet response after Mt. Pinatubo eruption.

3.5 Seasonal Plant Productivity Inferences plant productivity inferences

SMDI (at depths of 0-2; (0.6m), 2-4; (0.6m-1.2m), and 4-6 feet) (1.2m-1.6m)) and ETDI have proven helpful in analyzing the climatic impact of the Mt. Pinatubo eruption on a seasonal scale. Additionally, SMDI_2 (top 2 feet or 0.6 m) and ETDI have demonstrated elements a slow development of drought conditions, beginning by the end of the year 1991 (SON season), reflecting a time lag between seasonal precipitation on a seasonal scalepatterns (Narasimhan and

Srinivasan 2005). Crucially, the seasonal depiction of drying/wet conditions via SMDI and ETDI provides a comprehensive overview of prolonged or recurrent dry/wet conditions in susceptible regions. Moreover, understanding these typical agricultural drought indices indicates potential effects on plant productivity at the seasonal scale.

explored regions. In equatorial Africa, decreases in both SMDI and ETDI indicated that there was likely a negative impact on plant productivity. On the contrary, the The Mediterranean region (encompassing the eastern Mediterranean and western Asian region) showed increases imincreased SMDI and ETDI, indicating a positive effect on plant productivity. Northern Asia, on the other hand, exhibited an increase in SMDI with a decrease in ETDI, indicating suggesting that plant productivity likely decreased, but not because of water-based drivers.

3.6 High Frequency Impact Pathway Evaluation frequency impact pathways evaluation

Here, we use the daily model output on a daily scale to calculate weekly drought indices in each grid cell. These weekly scale drought indices and changes in other atmospheric variables are explored at the regional scale to understand the associated land-atmosphere interactions in terms of pertaining to higher-order impacts. High The higher temporal resolution of these parameters is crucial for analysis of analyzing different stages of the crop cycle in a region. Considering the complexity of the representation of spatial features, we selected three different distinct regions (shown in Figure 87 and detailed in Table 2 caption) in the northern hemisphere based on the

climate response to Mt. Pinatubo in the seasonal analyses presented in Section 3.0. - We

drought indices and atmospheric parameters.

followed the same strategy described in Section 2.3.1 to mask out the statistically insignificant

grid cells using the counterfactual ensemble after creating the weekly time series for different



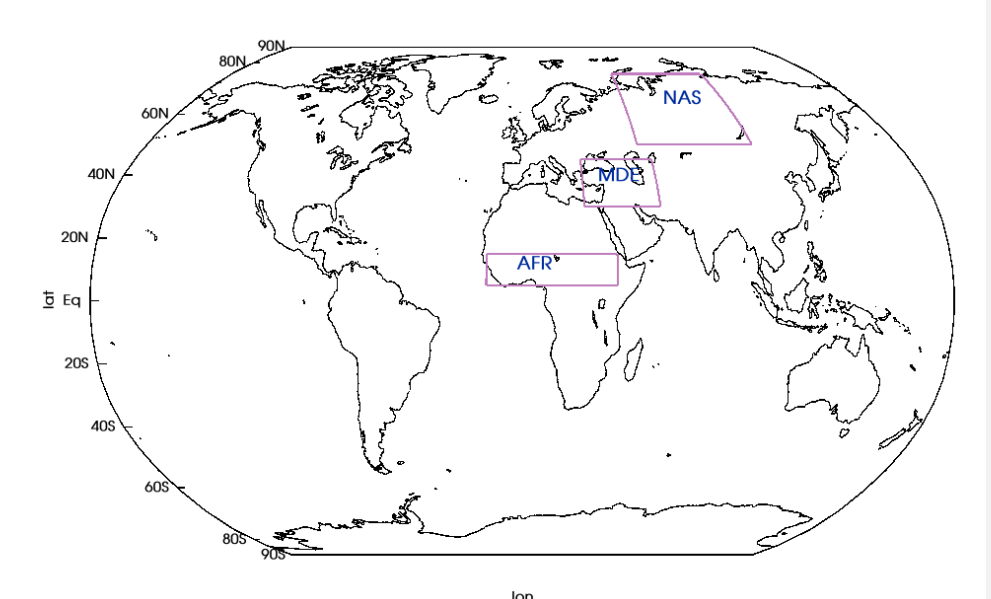


Figure 87: Demarcation of the regions selected over tropics, <u>Equatorial Africa Region</u> (AFR; <u>Lat: 5°N - 15°N</u>, <u>Lon: 15°W - 40°E</u>), mid-latitude, <u>Middle East Region</u> (MDE); <u>Lat: 30°N - 45°N</u>, <u>Lon: 27°E - 60°E</u>), and <u>in the high latitudes</u>, <u>Northern Asia Region</u> (NAS) as shown in table 2.; <u>Lat: 50°N - 75°N</u>, <u>Lon: 55°W - 110°E</u>).

Table 2. Table showing the details of regions demarcated to regional characteristics at a weekly scale.

Sr No.	Region Name	Region Stamp	Lat boundaries	Lon boundaries
1	Equatorial Africa Region	AFR	5° N 15° N	15° W - 40° E
2	Middle East Region	MDE	30° N - 45° N	27° E - 60° E
3	Northern Asia Region	NAS	50° N - 75° N	55° E - 110° E

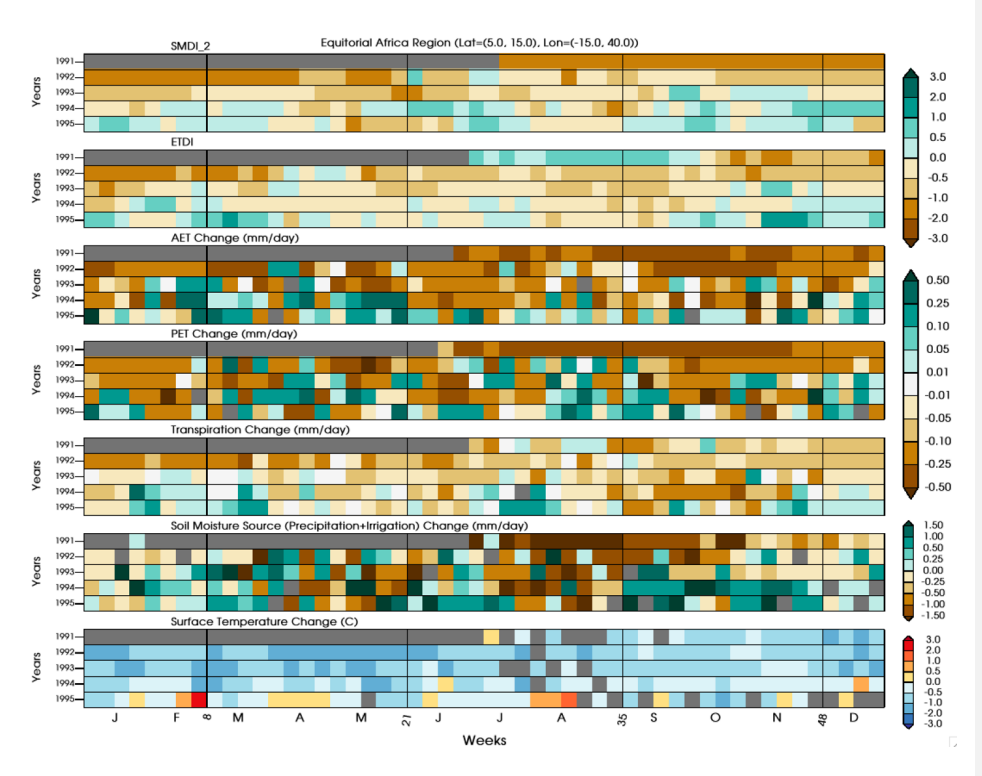


Figure 98. Spatially averaged drought indices (SMDI_2 & ETDI) and anomalies for other drivers (Surface Temperature, Precipitation plus irrigation, Actual and Potential Evapotranspiration, and Transpiration, Moisture Source (Precipitation plus irrigation) and Surface Temperature) at weekly scale for the equatorial Africa region (Latitude = 5°-15° N, Longitude = 15° W- 40° E).

3.6.1 Equatorial Africa

Figure 98 shows the weekly response to volcanic forcing for the years 1991-1995 in terms of agricultural drought indices (SMDI_2 & ETDI), <u>AET</u>, PET, <u>AET</u>, transpiration, total soil moisture source, and surface temperature for an equatorial region in northern Africa. This region exhibits consistent statistical differences across the drivers on a weekly scale-and; thus-, for most

of the majority of time periods are period, this is unmasked, revealing the degree of anomaly anomalous conditions.

698

699

700

701

702

703

704

705

706

707

708

709

710

711

712

713

714

715

716

717

718

719

720

This region lies between the latitude 5-15° N, where the precipitation during the monsoon season shows a decrease in response to a southern migration of the inter-tropical convergence zone in energetically deficit northern hemisphere due to volcanic aerosols preferentially reducing incoming radiation there (Iles et al., 2013; Colose et al., 2016; Singh et al., 2023). Weekly precipitation change in the equatorial African region Africa shows a significant deficit of more than 1.5 mm per day consistently for several weeks, especially during the JJAS monsoon season. This region also shows that a deficit in precipitation during the major precipitation season (JJAS) can result in a soil moisture deficit in the root zone in the following seasons (DJF and MAM in SMDI 2) and consequently affect the entire crop cycle. The root zone soil moisture, SMDI 2, also shows a persistent drying through 1993, and combined with the lack of precipitation, the potential for recharge is limited. Also, this region has no contribution from irrigation as a source of additional soil-moisture, as shown in figure S5Figure S7 (bottom panel) (Cook et al., 2020). Cumulative annual rainfall change over this region shows a deficit of 33.2, 9.5, and 3.2 mm per day for the yearyears 1991, 1992, and 1993 and an increase of 10.5 and 13.6 mm per day for the yearyears 1994 and 1995, respectively, where soil-moisture response shows a recovery from the dry conditions.

Hence, it is no surpriseunsurprising that there is a corresponding decrease in ETDI through 1993 that is consistent with this lack of moisture. However, the evaporative demand, as shown by surface temperature change, does not consistently decrease until September of 1991, and hence, ETDI is slow to show a decrease in the deficit index. After that point, evaporative demand decreases with lower temperatures contributing to a decrease in ETDI.

However, but the evapotranspiration is dominated by transpiration (Seneviratne et al 2010; Nilson and Assmann 2007-and references therein), and so the majority of the decrease in ETDI is explained by the shown decrease in plant transpiration. This As expected, this decrease in plant transpiration is, as expected, well correlated with decreases in AET.

Conclusively, precipitation response in this region shows dominance in regulating the ecohydrological conditions. A substantial decrease in the weekly rainfall over the region perpetuates a root-zone water deficit condition, resulting in decreased plant transpiration.

Decreases in both SMDI_2 and ETDI thus indicate the developing agricultural drought conditions, which are confirmed by a decrease in the direct measure of plant transpiration.

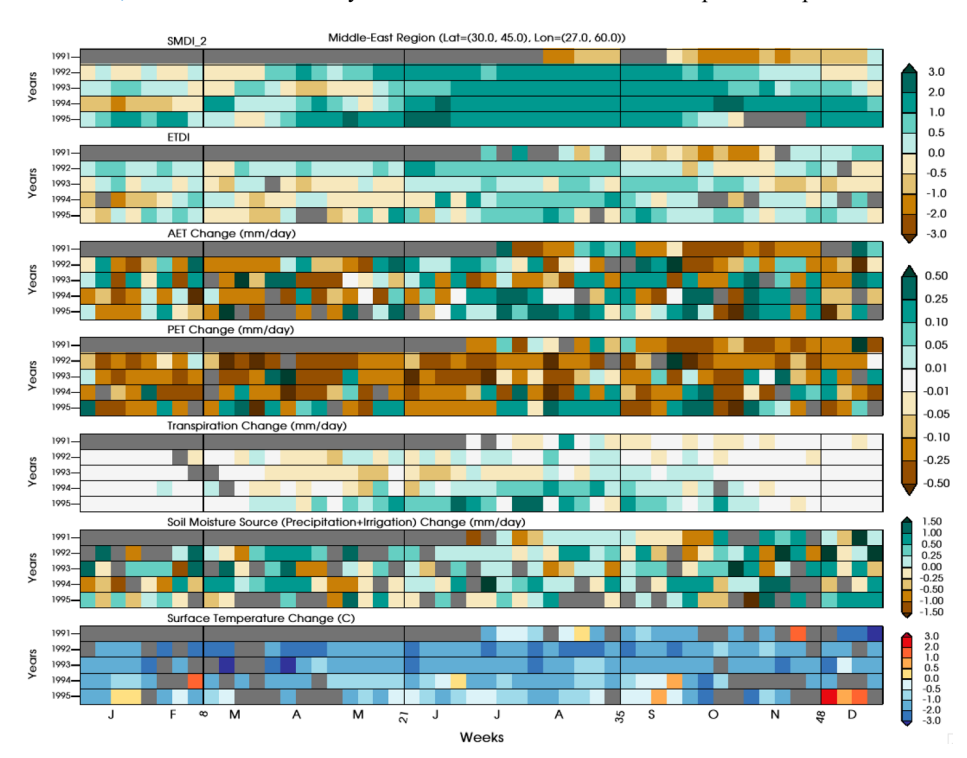


Figure 409. Spatially averaged drought indices (SMDI_2 & ETDI) and anomalies for other drivers (Surface Temperature, Precipitation plus irrigation, Actual and Potential Evapotranspiration, and Transpiration, Moisture Source (Precipitation plus irrigation) and Surface Temperature) at weekly scale for Middle East (MDE) Region (Latitude =30° N - 45° N,

Longitude=27°-60° E; easternEastern Mediterranean /-westernWestern Asian).

3.6.2 Middle East Region

Figure 109 shows the region covering the eastern Mediterranean and the western Asian regionregions where rainfall shows a slight increases lightly increased after the Mt. Pinatubo eruption. Additionally, this region exhibits a significantly positive trend in the irrigation practices post-10501950, with a substantial peak over the eastern Mediterranean region following the Mt. Pinatubo eruption (Cook et al., 2020; Figure 1 and 2).

In the eastern Mediterranean, wet and cold autumns and winters persist for several years after the Mt. Pinatubo eruption, offering significant root zone recharge potential. The summer months, in general, reflect a slightly uncertain model response in the regional rainfall, with some weeks of deficit and some of excess, but an additional water supply of water through the irrigation contributes to the overall moisture content in the region (Figure S5S7). Root zone soil moisture, (SMDI_2, shows ample-) indicates sufficient water duringavailability throughout the growing seasons throughduring the entire analysis period. Taken together, it is clearOverall, the findings demonstrate that this region is not moisture-limited and there is sufficient, with adequate precipitation and irrigation supply to recharge ensuring the replenishment of root zone moisture as plants grow. Cumulative weekly anomalies show that precipitation change in 1991 is slightly negative (-0.5 mm per day)), but an increase in annual rainfall of 13.8, 8.0, 10.9, and 4.5 mm per day is simulated for the yearycars 1992, 1993, 1994, and 1995, respectively.

Implemented irrigation overIrrigation implemented across this middle east Middle East region showsexhibits a strong positive trend for the periodfrom 1950-to 2005 (Cook et al., 2020), and).

Notably, a substantial significant cumulative increase in irrigation of 0.5, 1.3, 1.3, 0.8, and 0.9 mm per day in the irrigation for during the years 1991 to 1995 serves as the provides an additional source of moisture supply overfor the region (Cook et al., 2020). Thus, This irrigation supplies water especially inis particularly crucial during the summer months when compensating for rainfall change shows a few deficits lasting several weeks of deficit and contributes contributing 10–20% of the soil-moisture source change (Figure \$557).

The corresponding increases in ETDI and AET reflectindicate the ample source of abundant water availableavailability for transpiration in the region. Transpiration is againWhile transpiration remains temporally correlated with AET, but the increases are less well pronounced. At the same timeSimultaneously, there is a decreasedecline in PET response correlated, which is associated with the stronger a more significant temperature decrease in temperature in this region as compared to equatorial Africa. The decreasereduction in PET coupled, combined with the increase or maintenance inof AET (through transpiration) combine, leads to resultan increase in this region as there is is generally positively impacted, as ample moisture to provides essential support it. However, there are still heterogenous. Nevertheless, the data reveals heterogeneous patterns in this data showing, indicating that 1993, for instance, may have had some impact on influenced plant productivity with a positive but lower—magnitude ETDI, inconsistent AET, and decreased reduced transpiration.

Regardless of the presence of <u>a</u> volcanically induced response <u>or not</u>, the weekly scale analysis demonstrates its importance by virtue of an example from <u>the year 1993</u>, where rainfall deficit is produced during the 15th, and 16th weeks (April) of the year. Combined with <u>lowlower</u> SMDI 2, this <u>could result in a lack of may lead to insufficient</u> moisture availability during a

erucialcritical stage of the crop cycle. Given the The duration, this of such moisture deficits could significantly influence the impact overall seasonal crop production. Thus Consequently, even if the majority of the crop cycle possess favorable conditions, negative impacts at prevail for most of the crop cycle, adverse effects during essential phases of the crop cycle can crucially affect production critically influence yields in ways that seasonal averages would be unablefail to reveal capture.

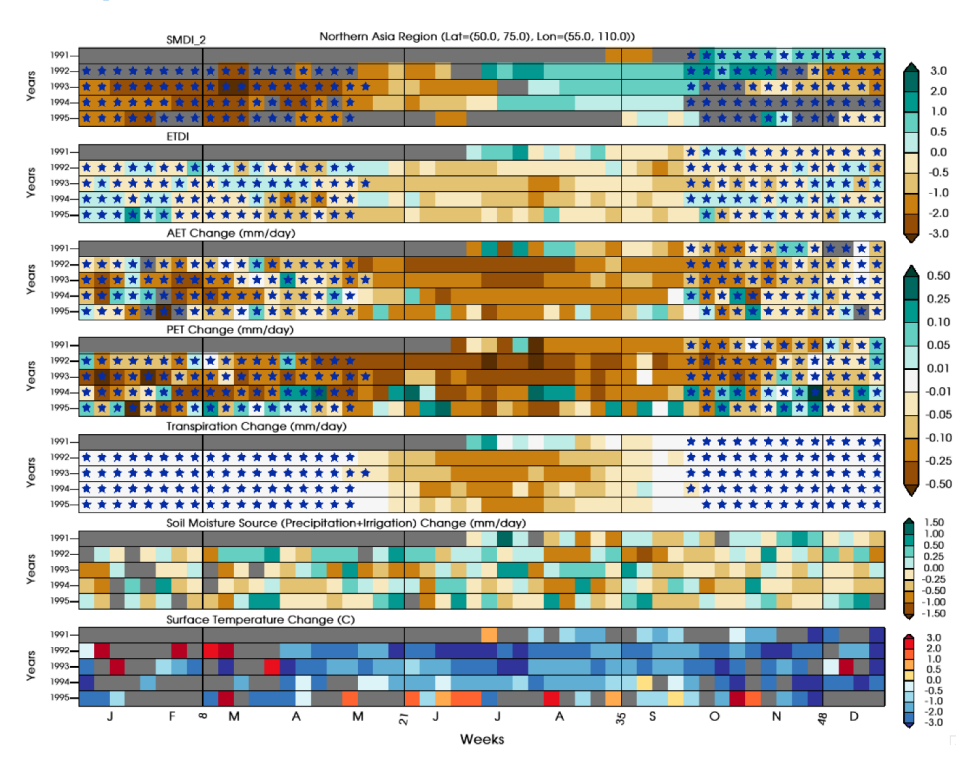


Figure 44_10. Spatially averaged drought indices (SMDI_2 & ETDI) and anomalies for other drivers (Surface Temperature, Precipitation plus irrigation, Actual and Potential Evapotranspiration, and Transpiration, Moisture Source (Precipitation plus irrigation) at weekly scale Northern Asia Region (Latitude =50° N - 75° N, Longitude=55°- 110° E). Blue stars represent the weeks with average surface temperature below freezing point.

3.6.3 Northern Asia

Finally, we selected a region (NAS) in higher latitudes to explore the interplay between the various drivers governing the conditions for plant productivity. Again, this This region consistently exhibits consistent statistical statistically significant differences across the drivers on a weekly scale. However, with higher latitudes also comes experience strong seasonal controls over on plant productivity, with below—freezing temperatures, shown with (indicated by blue stars,) halting productivity. Hence growth. Therefore, our analysis here will focus focuses on months during which plants can grow when plant growth is possible (~MJJAS).

Precipitation changes are highly uncertain over the entire analysis period, but in general are highly uncertain. However, there is generally a slight trend towardstoward increased precipitation from NovNovember 1991-to June 1992, followed by decreased precipitationa decline through 1994. As shown in FigFigure S5, the irrigation contribution of irrigation to soil moisture in this region is negligible. Cumulative weekly precipitation anomalies showindicate an annual increase of 0.05 mm per day for yearin 1991 and decrease, followed by decreases of -2.0, -4.1, -6.8, and -1.0 mm per day for the yearsfrom 1992 to 1995, respectively. Alternatively, root zone moisture shows amplethat sufficient water available to plants during the JAS (July-August-September) growing months after a strongsubstantial deficit in the early MJ (May-June) months.- Certainly, in these during the summer months, the melting of frozen surfaces and snow supplies moisture into the upper layers to become, resulting in wet accounting conditions, which accounts for this strong dichotomy.

However, there are notwere no corresponding increases in ETDI and AET afterfollowing the 1991 season.- This indicates that even though there is despite ample water, plants are still not growing; this is conclusively confirmed by the decrease in transpiration starting in 1992.

Meanwhile, the simultaneous decrease in reduction of PET response is correlated with the strongest decreasemost substantial decline in temperature, on the order of 2-3° C, for the three regions this region.

Unlike the other two regions for which SMDI_2 and ETDI exhibited similar wet/dry patterns, this locationregion shows diverging patterns. BroadlyOverall, this reveals indicates that even though there is although moisture is available to support plant productivity, the moisture it is not being effectively utilized. HenceTherefore, other factors must be responsible for the cause of decreased decrease in plant transpiration and ETDI. The stronger decrease of more significant decline in PET compared to AET indicates suggests that temperature may be playing a role here. Temperature. Since temperature is a direct proxy of decreased directly related to reduced incident radiation. Hence, the combined effects of temperature and radiation effects are likely the most important controls on decreased primary factors controlling the reduced plant productivity in this region, not rather than moisture conditions.

830 4.0 Conclusions

This study has used the Earth system modelling framework to explore the mechanisms by which the 1991 Mt. Pinatubo eruption affected the hydroclimatic conditions and water-based drivers of plant productivity. NASA GISS ModelE2.1 with the interactive chemistry and aerosol microphysical module (MATRIX) has demonstrated a successful simulation of microphysical properties (effective radius of order ~0.5 µm, aerosol extinction of ~0.21) of volcanic aerosol with induced radiative effect of longwave, shortwave, and net forcing of order of +3 Wm⁻², 8 Wm⁻² and -5 Wm⁻² respectively. This is consistent with the observations and other estimates (Russell et al., 1996; Bingen et al., 2004; Stenchikov et al., 1998; Bauman et al., 2003, Lacis et

al., 1992, Lacis 2015; Stenchikov et al., 1998; Hansen et al., 1992; Minnis et al., 1993; Brown et al 2024). The temperature response pathway shows Mt. Pinatubo eruption affected global surface cooling by ~0.5 °C with corresponding tropical lower stratosphere warming of 2-3 °C for several years after the eruption. This is consistent with the observations and other modeling estimates (Hansen et al., 1996; Parker et al., 1996; Stenchikov et al., 1998; Minnis et al., 1993; Kirchner et al., 1999; Ramachandran et al., 2000; Dutton and Christy 1992; Brown et al 2024). The GISS model simulates regional patches of decreases in rainfall of the order of 1 mm per day over the tropics and northern hemisphere regions (consistent with Joseph and Zheng, 2011; Liu et al., 2016; Trenberth and Dai, 2007), but the overall response of rainfall is highly uncertain. This study has endeavored to explore the secondary impacts of a volcanic eruption beyond the changes in radiation and temperature by examining agricultural drought indices to better infer impacts to plant productivity. Droughts are among the prime factors affecting regional crop yield at any stage of the crop cycle (Ben Abdelmalek and Nouiri, 2020; Leng and Hall, 2019; Raman et al., 2012). Both SMDI and ETDI represent the developing short- and longer-term conditions which support plant productivity, especially for agricultural applications. SMDI represents excess/deficit of soil moisture in different layers, whereas ETDI represents the active interaction between the land and atmosphere under perturbed climate conditions. An increase in the gap between the potential evapotranspiration (PET) and actual evapotranspiration (AET) represents the increased water stress condition either by increased potential evapotranspiration (water demand) or by the decrease in water available for evapotranspiration (lower AET). These drought indices confirm the moisture source based dry and wet pattern in early 1992 and the following years over the tropical and northern hemispheres mid-latitude regions correspondingly as a response to the volcanic forcings due to the Mt. Pinatubo eruption. Using both drought

839

840

841

842

843

844

845

846

847

848

849

850

851

852

853

854

855

856

857

858

859

860

indices, we conclude that approximately 10-15% of land region shows statistically significant dry or wet patterns in the volcanically perturbed climate conditions for 1992 and 1993. The fraction of land region showing a significant dry or wet response range between 5-10% for the next two (1994 and 1995) years. Broadly, the seasonal responses uncovered interesting behavior in three regions which we explore more deeply. In equatorial Africa, decreases in both SMDI and ETDI indicated that there was likely a negative impact on plant productivity while in a contrary manner the Middle East region showed increases in SMDI and ETDI indicating a positive impact on plant productivity. Northern Asia in comparison exhibited an increase in SMDI with a decrease in ETDI indicating that plant productivity likely decreased, but not because of water-based drivers.

Using This study utilized the NASA GISS ModelE2.1 (MATRIX) Earth system modeling framework to investigate the mechanisms by which the 1991 Mt. Pinatubo eruption influenced hydroclimatic conditions and water-based drivers of plant productivity. The simulation successfully reproduced key microphysical properties ($R_{eff} \approx 0.5 \, \mu m$, AOD ≈ 0.22), radiative forcing (\sim -5 Wm $^{-2}$), surface cooling (\sim 0.5°C), and regional rainfall changes consistent with previous studies. The study further examined secondary impacts of the eruption, beyond changes in radiation and temperature, by analyzing agricultural drought indices to better assess its effects on plant productivity. Two metrics, SMDI and ETDI, which account for land-atmosphere interactions, were utilized to capture the progression of short- and long-term conditions affecting plant productivity, particularly in agricultural contexts. These drought indices confirm the moisture-driven dry and wet patterns observed in early 1992 and the following years over the tropical regions and mid-latitudes of the Northern Hemisphere, respectively, as a response to the radiative perturbation caused by the Mt. Pinatubo eruption. Based on both drought indices, we

conclude that approximately 10-15% of land areas exhibit statistically significant dry or wet patterns under the volcanically altered climate conditions of 1992 and 1993. The fraction of land region showing a significant dry or wet response range between 5-10% for the next two (1994 and 1995) years. In equatorial Africa, seasonal decreases in both SMDI and ETDI suggested a likely negative impact on plant productivity. In contrast, the Middle East showed increases in both SMDI and ETDI, indicating a positive effect on plant productivity. Northern Asia, by comparison, exhibited an increase in SMDI alongside a decrease in ETDI, implying a reduction in plant productivity, though not driven by water-related factors.

Motivated by these key pattern differences as motivation, we deepenedextended our analysis of thesethe drought indices usingby incorporating higher temporal (weekly) frequencies and by incorporating along with AET, PET, and transpiration-directly. In general, these. These regional analyses possessgenerally exhibit much stronger statistical significance on thea weekly scale; and they further confirmedconfirm the seasonally season-based inferences described above.— Further, weekly drought indices show the temporal variability characteristics in the signal, which also demonstrates the utility of explaining the effectiveness of short-term dry/wet conditions corresponding to a regional crop cycle.— In locations where there is with insufficient/excess soil moisture, there is a corresponding decrease/increase in evapotranspiration (AFR/MDE) and hence decreased/increased plant productivity.

Kandlbauer et al., (2013) examined crop responses (using C3 and C4 grasses as proxies) to the 1815 Tambora eruption using the HadGEM-ES model in three regions very similar to those in our study. Their findings suggest that plant productivity decreases with positive changes in soil moisture in the higher-latitude Asian region. In the mid-latitudes over the Southern Europe/Middle East region (adjacent to our MDE region), volcanic eruptions may enhance plant

productivity by providing additional soil moisture through increased rainfall. However, in the MDE region in our study, we found that the applied irrigation also benefits soil moisture supply along with the increased rainfall. Furthermore, both studies report a decrease in productivity in the tropical region. In general, these results complement the findings of this study, which suggest that if sufficient water is available in the Southern Europe/Middle East region, volcanic eruptions may enhance plant productivity. In contrast, in the far northern latitudes, water is not the primary driver of plant responses, and productivity is likely to decline. Seasonal-scale changes in gross primary productivity (GPP) confirm the regional trends in plant productivity following the eruption. The simulations show a more pronounced decrease in GPP in the northern high-latitude region and a significant increase in GPP over the European and Mediterranean regions.

Additionally, distinct patterns of decrease and increase in GPP are simulated in the tropical northern and southern regions, respectively (Figure S9).

This workstudy is the first to conclusively showdemonstrate that there is an excess of root-zone soil moisture in high-latitudes—latitude regions (NAS) which is not being utilized bythat plants to grow establishing the main control is likely are not utilizing for growth, indicating that temperature and radiation basedare likely the primary controlling factors, thus confirming the results of previous findings (Krakauer and Randerson, 2003) and (Dong and Dai, 2017). The intricate nature of the compounded response, particularly regarding the in relation to soil moisture-baseddriven impact pathways in tropical regions and higher latitudes acrosshigh-latitude areas of the Northern Hemisphere, highlights the northern hemisphere, also underscores the necessity of broadening the scope of need to expand the investigation beyond soil moisture and land-atmosphere interactions. The current setupconfiguration of the NASA GISS model effectively runs using operates with prescribed vegetation with static plant functional types and

leaf area index, and the inclusion of. Incorporating dynamic vegetation could be erucial essential for addingcapturing interactive land surface responses. Also, assessing Additionally, evaluating the influence of the regional and local biomebiomes on photosynthesis raterates could provide a more detailed understanding of offer deeper insights into how these processes specifically respond to the climate impact climatic impacts of volcanic forcings. McDermid et al. (2022) have demonstrated the sensitivity of regional hydroclimate to the local changes in soil organic carbon changes using the soil moisture content. The results presented in this study in terms of regarding soil-moisture-based drivers to the plant productivity and surface temperature response in the northern hemispherehemisphere's high latitudes also hinthinted towards the dominance of temperature effects on enhanced carbon sink in terms of soil and plant respiration and reduced NPP (Krakauer and Randerson, 2003; Lucht et al., 2002). Meanwhile, water-based drivers dominatepredominantly influence productivity responses in multiplemany tropical and subtropicalsubtropical regions. Our results illustrate findings demonstrate that soil-moisture-based conditions in theacross different regions can be useful for evaluating and understanding provide valuable insights into the full impacts on the agricultural yieldyields and regional carbon sink response if the responses, particularly under scenarios involving changes in dynamic vegetation and crop cover-changes. A recently developed fully demographic dynamic vegetation model (ModelE-BiomE v.1.0 (Weng et al., 2022)) withincorporates interactive biophysical and biogeochemical feedback feedbacks between climate and land systems for within the NASA GISS ModelE framework. This model could be helpfulinstrumental in evaluating the carbon cycle responseresponses under such forcings. Code/Data availability. Details to support the results in the manuscript is available as supplementary information is

931

932

933

934

935

936

937

938

939

940

941

942

943

944

945

946

947

948

949

950

951

952

953

954

provided with the manuscript. GISS Model code snapshots are available at

- 955 https://simplex.giss.nasa.gov/snapshots/ (National Aeronautics and Space Administration, 2024)
- 956 and calculated diagnostics are available at zenodo repository
- 957 (https://zenodo.org/records/12734905) (Singh et al., 2024). However, raw model output and data
- 958 at high temporal (daily) resolution and codes are available on request from author due to large data
- 959 volume.

960 Acknowledgements

- 961 Resources supporting this work were provided by the NASA High-End Computing (HEC)
- 962 Program through the NASA Center for Climate Simulation (NCCS) at Goddard Space Flight
- 963 Center. The authors thank Ben I Cook, Nancy Y Kiang, Igor Aleinov and Michael Puma for their
- 964 input through multiple discussions with the project members. RS, KT, DB, LS, BW, and KM were
- 965 supported by the Laboratory Directed Research and Development program at Sandia National
- 966 Laboratories, a multi-mission laboratory managed and operated by National Technology and
- 967 Engineering Solutions of Sandia LLC, a wholly owned subsidiary of Honeywell International Inc.
- 968 for the U.S. Department of Energy's National Nuclear Security Administration under contract DE-
- 969 NA0003525. This paper describes objective technical results and analysis. Any subjective views
- 970 or opinions that might be expressed in the paper do not necessarily represent the views of the U.S.
- 971 Department of Energy or the United States Government.

972 Author's contributions

- 973 RS, KT, DB, LS and KM identified the study period in consultation with the other authors and RS,
- 974 KT, DB, LS and BW designed the underlying simulations strategies. RS and KT implemented it
- 975 and performed the simulations using NASA GISS ModelE. RS and KT have performed the
- analysis. RS created the figures in close collaboration with all authors. RS wrote the first draft of
- 977 the manuscript, and all other authors has contributed the writing of subsequent drafts. All authors
- 978 contributed to the interpretation of results.

979 Competing interests

- 980 One of the co-authors is member of the editorial board of Atmospheric Chemistry and Physics.
- 981 Short Summary
- 982 Analysis of post-eruption climate conditions using the impact metrics is crucial for understanding
- 983 the hydroclimatic responses. We used NASA's Earth system model to perform the experiments and
- 984 utilize the moisture-based impact metrics and hydrological variables to investigate the effect of

985	volcanically induced conditions that govern plant productivity. This study <u>demonstrates highlights</u>
986	the Mt. Pinatubo's impact of the Mt. Pinatubo eruption on the drivers of plant productivity and, as
987	well as the regional and seasonal dependence of different these drivers.
988	
989	Reference:
990	Allen, R.G., Pereira, L.S., Raes, D., et al. (1998) Crop Evapotranspiration-Guidelines for
991	Computing Crop Water Requirements-FAO Irrigation and Drainage Paper 56. FAO, Rome, 300(9):
992	D05109 .
993	Aquila, V., Oman, L. D., Stolarski, R. S., Colarco, P. R., and Newman, P. A.: Dispersion of the
994	volcanic sulfate cloud from a Mount Pinatubo like eruption, Journal of Geophysical Research:
995	Atmospheres, 117, https://doi.org/10.1029/2011JD016968, 2012.
996	Barnes, E. A., Solomon, S., and Polvani, L. M.: Robust Wind and Precipitation Responses to the
997	Mount Pinatubo Eruption, as Simulated in the CMIP5 Models, Journal of Climate, 29, 4763–
998	4778, https://doi.org/10.1175/JCLI-D-15-0658.1, 2016.
999	Barnes, J. E. and Hofmann, D. J.: Lidar measurements of stratospheric aerosol over Mauna Loa
1000	Observatory, Geophysical Research Letters, 24, 1923–1926,
1001	https://doi.org/10.1029/97GL01943, 1997.
1002	Bauer, S. E., Wright, D. L., Koch, D., Lewis, E. R., McGraw, R., Chang, LS., Schwartz, S. E., and
1003	Ruedy, R.: MATRIX (Multiconfiguration Aerosol TRacker of mIXing state): an aerosol
1004	microphysical module for global atmospheric models, Atmospheric Chemistry and Physics, 8,
1005	6003 6035, https://doi.org/10.5194/acp 8 6003 2008, 2008.
1006	Bauer, S. E., Ault, A., and Prather, K. A.: Evaluation of aerosol mixing state classes in the GISS
1007	modelE MATRIX climate model using single particle mass spectrometry measurements, Journal
1008	of Geophysical Research: Atmospheres, 118, 9834–9844, https://doi.org/10.1002/jgrd.50700,
1009	2013.
1010	Bauer, S. E., Tsigaridis, K., Faluvegi, G., Kelley, M., Lo, K. K., Miller, R. L., Nazarenko, L., Schmidt,
1011	G. A., and Wu, J.: Historical (1850–2014) Aerosol Evolution and Role on Climate Forcing Using
1012 1013	the GISS ModelE2.1 Contribution to CMIP6, Journal of Advances in Modeling Earth Systems, 12, e2019MS001978, https://doi.org/10.1029/2019MS001978, 2020.
1013	C2015Wi3001578, https://doi.org/10.1025/2015Wi3001578, 2020.
1014	Bauman, J. J., Russell, P. B., Geller, M. A., and Hamill, P.: A stratospheric aerosol climatology from
1015	SAGE II and CLAES measurements: 2. Results and comparisons, 1984–1999, Journal of
1016	Geophysical Research: Atmospheres, 108, https://doi.org/10.1029/2002JD002993, 2003.
1017	Bekki, S.: Oxidation of volcanic SO2: A sink for stratospheric OH and H2O, Geophysical Research
1018	Letters, 22, 913–916, https://doi.org/10.1029/95GL00534, 1995.

1h10		Ben Abdelmalek, M. and Nouiri, I.: Study of trends and mapping of drought events in Tunisia
1019	7	ben Abdelmalek, W. and Nodin, I Study of trends and mapping of drought events in rumsia

- 1020 and their impacts on agricultural production, Science of The Total Environment, 734, 139311,
- 1021 https://doi.org/10.1016/j.scitotenv.2020.139311, 2020.
- 1022 Bingen, C., Fussen, D., and Vanhellemont, F.: A global climatology of stratospheric aerosol size
- 1023 distribution parameters derived from SAGE II data over the period 1984–2000: 1. Methodology
- 1024 and climatological observations, Journal of Geophysical Research: Atmospheres, 109,
- 1025 https://doi.org/10.1029/2003JD003518, 2004.
- 1026 Bluth, G. J. S., Doiron, S. D., Schnetzler, C. C., Krueger, A. J., and Walter, L. S.: Global tracking of
- the SO2 clouds from the June, 1991 Mount Pinatubo eruptions, Geophysical Research Letters,
- 1028 19, 151–154, https://doi.org/10.1029/91GL02792, 1992.
- 1029 Brad Adams, J., Mann, M. E., and Ammann, C. M.: Proxy evidence for an El Niño like response to
- 1030 volcanic forcing, Nature, 426, 274-278, https://doi.org/10.1038/nature02101, 2003-
- 1031 Briffa, K. R., Jones, P. D., Schweingruber, F. H., and Osborn, T. J.: Influence of volcanic cruptions
- 1032 on Northern Hemisphere summer temperature over the past 600 years, Nature, 393, 450–455,
- 1033 https://doi.org/10.1038/30943, 1998.
- 1034 Brown, H. Y., Wagman, B., Bull, D., Peterson, K., Hillman, B., Liu, X., Ke, Z., and Lin, L.: Validating
- 1035 a microphysical prognostic stratospheric acrosol implementation in E3SMv2 using the Mount
- 1036 Pinatubo eruption, EGUsphere, 1–46, https://doi.org/10.5194/egusphere-2023-3041, 2024.
- 1037 Carn, S. A., Fioletov, V. E., McLinden, C. A., Li, C., and Krotkov, N. A.: A decade of global volcanic
- 1038 SO2 emissions measured from space, Sci Rep, 7, 44095, https://doi.org/10.1038/srep44095,
- 1039 2017.
- 1040 Chen, D.-X. and Coughenour, M. B.: Photosynthesis, transpiration, and primary productivity:
- 1041 Scaling up from leaves to canopies and regions using process models and remotely sensed data,
- 1042 Global Biogeochemical Cycles, 18, https://doi.org/10.1029/2002GB001979, 2004.
- 1043 Colose, C. M., LeGrande, A. N., and Vuille, M.: Hemispherically asymmetric volcanic forcing of
- 1044 tropical hydroclimate during the last millennium, Earth System Dynamics, 7, 681–696,
- 1045 https://doi.org/10.5194/esd-7-681-2016, 2016.
- 1046 Cook, B. I., McDermid, S. S., Puma, M. J., Williams, A. P., Seager, R., Kelley, M., Nazarenko, L., and
- 1047 Aleinov, I.: Divergent Regional Climate Consequences of Maintaining Current Irrigation Rates in
- 1048 the 21st Century, Journal of Geophysical Research: Atmospheres, 125, e2019JD031814,
- 1049 https://doi.org/10.1029/2019JD031814, 2020.
- 1050 Denissen, J. M. C., Teuling, A. J., Pitman, A. J., Koirala, S., Migliavacca, M., Li, W., Reichstein, M.,
- 1051 Winkler, A. J., Zhan, C., and Orth, R.: Widespread shift from ecosystem energy to water
- 1052 limitation with climate change, Nat. Clim. Chang., 12, 677 684, https://doi.org/10.1038/s41558
- 1053 022-01403-8, 2022.

1054	Desilier, 1., hervig, Wr. E., hormann, D. J., kosen, J. Wr., and Eney, J. B., thirty years of in situ
1055	stratospheric acrosol size distribution measurements from Laramie, Wyoming (41°N), using
1006	halland barras instruments. Incomel of Combusinal Barrasab. Attacambarras, 100

- 1056 balloon borne instruments, Journal of Geophysical Research: Atmospheres, 108,
- 1057 https://doi.org/10.1029/2002JD002514, 2003.
- 1058 Dhomse, S. S., Emmerson, K. M., Mann, G. W., Bellouin, N., Carslaw, K. S., Chipperfield, M. P.,
- 1059 Hommel, R., Abraham, N. L., Telford, P., Braesicke, P., Dalvi, M., Johnson, C. E., O'Connor, F.,
- 1060 Morgenstern, O., Pyle, J. A., Deshler, T., Zawodny, J. M., and Thomason, L. W.: Aerosol
- 1061 microphysics simulations of the Mt.~Pinatubo eruption with the UM-UKCA composition-climate
- 1062 model, Atmospheric Chemistry and Physics, 14, 11221–11246, https://doi.org/10.5194/acp 14
- 1063 11221 2014, 2014.
- 1064 Dong, B. and Dai, A.: The uncertainties and causes of the recent changes in global
- 1065 evapotranspiration from 1982 to 2010, Clim Dyn, 49, 279–296, https://doi.org/10.1007/s00382
- 1066 016-3342-x, 2017.
- 1067 Dutton, E. G. and Christy, J. R.: Solar radiative forcing at selected locations and evidence for
- 1068 global lower tropospheric cooling following the eruptions of El Chichón and Pinatubo,
- 1069 Geophysical Research Letters, 19, 2313–2316, https://doi.org/10.1029/92GL02495, 1992.
- 1070 English, J. M., Toon, O. B., and Mills, M. J.: Microphysical simulations of large volcanic cruptions:
- 1071 Pinatubo and Toba, Journal of Geophysical Research: Atmospheres, 118, 1880–1895,
- 1072 https://doi.org/10.1002/jgrd.50196, 2013.
- 1073 Farquhar, G. D. and Roderick, M. L.: Pinatubo, Diffuse Light, and the Carbon Cycle, Science, 299,
- 1<mark>074 1997–1998, https://doi.org/10.1126/science.1080681, 2003.</mark>
- 1075 Fujiwara, M., Martineau, P., and Wright, J. S.: Surface temperature response to the major
- 1076 volcanic eruptions in multiple reanalysis data sets, Atmospheric Chemistry and Physics, 20, 345
- 1077 374, https://doi.org/10.5194/acp 20 345 2020, 2020.
- 1078 Gao, C. Y., Naik, V., Horowitz, L. W., Ginoux, P., Paulot, F., Dunne, J., Mills, M., Aquila, V., and
- 1079 Colarco, P.: Volcanic Drivers of Stratospheric Sulfur in GFDL ESM4, Journal of Advances in
- 1080 Modeling Earth Systems, 15, e2022MS003532, https://doi.org/10.1029/2022MS003532, 2023.
- 1081 Gao, F., Morisette, J. T., Wolfe, R. E., Ederer, G., Pedelty, J., Masuoka, E., Myneni, R., Tan, B., and
- 1082 Nightingale, J.: An Algorithm to Produce Temporally and Spatially Continuous MODIS-LAI Time
- 1083 Series, IEEE Geoscience and Remote Sensing Letters, 5, 60–64,
- 1084 https://doi.org/10.1109/LGRS.2007.907971, 2008.
- 1085 Gery, M. W., Whitten, G. Z., Killus, J. P., and Dodge, M. C.: A photochemical kinetics mechanism
- 1086 for urban and regional scale computer modeling, Journal of Geophysical Research:
- 1087 Atmospheres, 94, 12925–12956, https://doi.org/10.1029/JD094iD10p12925, 1989.

1088 1089 1090	Gu, G. and Adler, R. F.: Precipitation and Temperature Variations on the Interannual Time Scale: Assessing the Impact of ENSO and Volcanic Eruptions, Journal of Climate, 24, 2258–2270, https://doi.org/10.1175/2010JCLI3727.1, 2011.
1091 1092 1093	Gu, G. and Adler, R. F.: Large scale, inter annual relations among surface temperature, water vapour and precipitation with and without ENSO and volcano forcings, International Journal of Climatology, 32, 1782–1791, https://doi.org/10.1002/joc.2393, 2012.
1094 1095 1096	Gu, G., Adler, R. F., Huffman, G. J., and Curtis, S.: Tropical Rainfall Variability on Interannual-to- Interdecadal and Longer Time Scales Derived from the GPCP Monthly Product, Journal of Climate, 20, 4033–4046, https://doi.org/10.1175/JCLI4227.1, 2007.
1097 1098 1099	Gu, L., Baldocchi, D., Verma, S. B., Black, T. A., Vesala, T., Falge, E. M., and Dowty, P. R.: Advantages of diffuse radiation for terrestrial ecosystem productivity, Journal of Geophysical Research: Atmospheres, 107, ACL 2 1 ACL 2 23, https://doi.org/10.1029/2001JD001242, 2002.
1100 1101 1102	Gu, L., Baldocchi, D. D., Wofsy, S. C., Munger, J. W., Michalsky, J. J., Urbanski, S. P., and Boden, T. A.: Response of a Deciduous Forest to the Mount Pinatubo Eruption: Enhanced Photosynthesis, Science, 299, 2035–2038, https://doi.org/10.1126/science.1078366, 2003.
1103 1104 1105	Hane, D. C. and Pumphrey, F. V.: Yield evapotranspiration relationships and seasonal crop coefficients for frequently irrigated potatoes, American Potato Journal, 61, 661–668, https://doi.org/10.1007/BF02852929, 1984.
1106 1107 1108	Hansen, J., Lacis, A., Ruedy, R., and Sato, M.: Potential climate impact of Mount Pinatubo eruption, Geophysical Research Letters, 19, 215–218, https://doi.org/10.1029/91GL02788, 1992.
1109 1110 1111 1112 1113 1114	Hansen, J., Sato, M., Ruedy, R., Lacis, A., Asamoah, K., Borenstein, S., Brown, E., Cairns, B., Caliri, G., Campbell, M., Curran, B., de Castro, S., Druyan, L., Fox, M., Johnson, C., Lerner, J., McCormick, M. P., Miller, R., Minnis, P., Morrison, A., Pandolfo, L., Ramberrann, I., Zaucker, F., Robinson, M., Russell, P., Shah, K., Stone, P., Tegen, I., Thomason, L., Wilder, J., and Wilson, H.: A Pinatubo Climate Modeling Investigation, in: The Mount Pinatubo Eruption, Berlin, Heidelberg, 233–272, https://doi.org/10.1007/978-3-642-61173-5_20, 1996.
1115 1116 1117	Hansen, J. E., Lacis, A. A., Lee, P., and Wang, W. C.: Climatic Effects of Atmospheric Aerosols, Annals of the New York Academy of Sciences, 338, 575–587, https://doi.org/10.1111/j.1749-6632.1980.tb17151.x, 1980.
1118 1119 1120	Hao, Z., Xiong, D., Zheng, J., Yang, L. E., and Ge, Q.: Volcanic eruptions, successive poor harvests and social resilience over southwest China during the 18–19th century, Environ. Res. Lett., 15, 105011, https://doi.org/10.1088/1748-9326/abb159, 2020.

Hitchman, M. H., McKay, M., and Trepte, C. R.: A climatology of stratospheric aerosol, J. Geophys.

Res.-Atmos., 99, 20689-20700, https://doi.org/10.1029/94JD01525, 1994.

Hoesly, R. M., Smith, S. J., Feng, L., Klimont, Z., Janssens Maenhout, G., Pitkanen, T., Seibert, J. J., 1125 Vu, L., Andres, R. J., Bolt, R. M., Bond, T. C., Dawidowski, L., Kholod, N., Kurokawa, J., Li, M., Liu, 1126 L., Lu, Z., Moura, M. C. P., O'Rourke, P. R., and Zhang, Q.: Historical (1750 2014) anthropogenic 1127 emissions of reactive gases and aerosols from the Community Emissions Data System (CEDS), 1128 Geoscientific Model Development, 11, 369-408, https://doi.org/10.5194/gmd-11-369-2018, 1129 2018. 1130 Huhtamaa, H. and Helama, S.: Distant impact: tropical volcanic eruptions and climate-driven 1131 agricultural crises in seventeenth-century Ostrobothnia, Finland, Journal of Historical 1132 Geography, 57, 40-51, https://doi.org/10.1016/j.jhg.2017.05.011, 2017. 1133 lles, C. E., Hegerl, G. C., Schurer, A. P., and Zhang, X.: The effect of volcanic eruptions on global 1134 precipitation, Journal of Geophysical Research: Atmospheres, 118, 8770-8786, 1135 https://doi.org/10.1002/jgrd.50678, 2013. 1136 Ito, G., Romanou, A., Kiang, N. Y., Faluvegi, G., Aleinov, I., Ruedy, R., Russell, G., Lerner, P., Kelley, 1137 M., and Lo, K.: Global Carbon Cycle and Climate Feedbacks in the NASA GISS ModelE2.1, Journal of Advances in Modeling Earth Systems, 12, e2019MS002030, 1138 1139 https://doi.org/10.1029/2019MS002030, 2020. 1140 Jones, C. D. and Cox, P. M.: Modeling the volcanic signal in the atmospheric CO2 record, Global 1141 Biogeochemical Cycles, 15, 453-465, https://doi.org/10.1029/2000GB001281, 2001. 1142 Joseph, R. and Zeng, N.: Seasonally Modulated Tropical Drought Induced by Volcanic Aerosol, 1143 Journal of Climate, 24, 2045-2060, https://doi.org/10.1175/2009JCLI3170.1, 2011. 1144 Kelley, M., Schmidt, G. A., Nazarenko, L. S., Bauer, S. E., Ruedy, R., Russell, G. L., Ackerman, A. S., 1145 Aleinov, I., Bauer, M., Bleck, R., Canuto, V., Cesana, G., Cheng, Y., Clune, T. L., Cook, B. I., Cruz, C. 1146 A., Del Genio, A. D., Elsaesser, G. S., Faluvegi, G., Kiang, N. Y., Kim, D., Lacis, A. A., Leboissetier, 1147 A., LeGrande, A. N., Lo, K. K., Marshall, J., Matthews, E. E., McDermid, S., Mezuman, K., Miller, R. 1148 L., Murray, L. T., Oinas, V., Orbe, C., García Pando, C. P., Perlwitz, J. P., Puma, M. J., Rind, D., 1149 Romanou, A., Shindell, D. T., Sun, S., Tausnev, N., Tsigaridis, K., Tselioudis, G., Weng, E., Wu, J., 1150 and Yao, M. S.: GISS-E2.1: Configurations and Climatology, Journal of Advances in Modeling Earth Systems, 12, e2019MS002025, https://doi.org/10.1029/2019MS002025, 2020. 1151 1152 Keshavarz, M. R., Vazifedoust, M., and Alizadeh, A.: Drought monitoring using a Soil Wetness 1153 Deficit Index (SWDI) derived from MODIS satellite data, Agricultural Water Management, 132, 37-45, https://doi.org/10.1016/j.agwat.2013.10.004, 2014. 1154 1155 Kiehl, J. T. and Trenberth, K. E.: Earth's Annual Global Mean Energy Budget, Bulletin of the 1156 American Meteorological Society, 78, 197-208, https://doi.org/10.1175/1520-1157 0477(1997)078<0197:EAGMEB>2.0.CO:2. 1997.

1124

1158

1159

Kim, Y., Moorcroft, P. R., Aleinov, I., Puma, M. J., and Kiang, N. Y.: Variability of phenology and

fluxes of water and carbon with observed and simulated soil moisture in the Ent Terrestrial

1160 1161	Biosphere Model (Ent TBM version 1.0.1.0.0), Geoscientific Model Development, 8, 3837–3865, https://doi.org/10.5194/gmd-8-3837-2015, 2015.
1162 1163 1164	Kinne, S., Toon, O. B., and Prather, M. J.: Buffering of stratospheric circulation by changing amounts of tropical ozone—a Pinatubo case study, Geophysical Research Letters (American Geophysical Union); (United States), 19:19, https://doi.org/10.1029/92GL01937, 1992.
1165 1166 1167	Krakauer, N. Y. and Randerson, J. T.: Do volcanic eruptions enhance or diminish net primary production? Evidence from tree rings, Global Biogeochemical Cycles, 17, https://doi.org/10.1029/2003GB002076, 2003.
1168 1169 1170	Labitzke, K. and McCormick, M. P.: Stratospheric temperature increases due to Pinatubo aerosols, Geophysical Research Letters, 19, 207–210, https://doi.org/10.1029/91GL02940, 1992.
1171 1172	Lacis, A.: Volcanic aerosol radiative properties, PAGES Mag, 23, 50–51, https://doi.org/10.22498/pages.23.2.50, 2015.
1173 1174	Lacis, A., Hansen, J., and Sato, M.: Climate forcing by stratospheric aerosols, Geophysical Research Letters, 19, 1607–1610, https://doi.org/10.1029/92GL01620, 1992.
1175 1176 1177	Lacis, A. A. and Hansen, J.: A Parameterization for the Absorption of Solar Radiation in the Earth's Atmosphere, Journal of the Atmospheric Sciences, 31, 118–133, https://doi.org/10.1175/1520_0469(1974)031<0118:APFTAO>2.0.CO;2, 1974.
1178 1179 1180	Lambert, A., Grainger, R. G., Remedios, J. J., Rodgers, C. D., Corney, M., and Taylor, F. W.: Measurements of the evolution of the Mt. Pinatubo aerosol cloud by ISAMS, Geophysical Research Letters, 20, 1287–1290, https://doi.org/10.1029/93GL00827, 1993.
1181	LeGrande, A. N. and Anchukaitis, K. J.: Volcanic eruptions and climate, 23, 2015.
1182 1183 1184	LeGrande, A. N., Tsigaridis, K., and Bauer, S. E.: Role of atmospheric chemistry in the climate impacts of stratospheric volcanic injections, Nature Geosci, 9, 652–655, https://doi.org/10.1038/ngeo2771, 2016.
1185 1186 1187	Leng, G. and Hall, J.: Crop yield sensitivity of global major agricultural countries to droughts and the projected changes in the future, Science of The Total Environment, 654, 811–821, https://doi.org/10.1016/j.scitotenv.2018.10.434, 2019.
1188 1189 1190	Li, J., Xie, SP., Cook, E. R., Morales, M. S., Christie, D. A., Johnson, N. C., Chen, F., D'Arrigo, R., Fowler, A. M., Gou, X., and Fang, K.: El Niño modulations over the past seven centuries, Nature Clim Change, 3, 822–826, https://doi.org/10.1038/nclimate1936, 2013.
1191 1192 1193	Liu, F., Chai, J., Wang, B., Liu, J., Zhang, X., and Wang, Z.: Global monsoon precipitation responses to large volcanic eruptions, Sci Rep, 6, 24331, https://doi.org/10.1038/srep24331, 2016.

1194 1195 1196	Lobell, D. B. and Field, C. B.: Global scale climate—crop yield relationships and the impacts of recent warming, Environ. Res. Lett., 2, 014002, https://doi.org/10.1088/1748-9326/2/1/014002, 2007.
1197 1198 1199	Lucht, W., Prentice, I. C., Myneni, R. B., Sitch, S., Friedlingstein, P., Cramer, W., Bousquet, P., Buermann, W., and Smith, B.: Climatic Control of the High-Latitude Vegetation Greening Trend and Pinatubo Effect, Science, 296, 1687–1689, https://doi.org/10.1126/science.1071828, 2002.
1200 1201 1202	Manning, J. G., Ludlow, F., Stine, A. R., Boos, W. R., Sigl, M., and Marlon, J. R.: Volcanic suppression of Nile summer flooding triggers revolt and constrains interstate conflict in ancient Egypt, Nat Commun, 8, 900, https://doi.org/10.1038/s41467-017-00957-y, 2017.
1203 1204 1205 1206 1207 1208	van Marle, M. J. E., Kloster, S., Magi, B. I., Marlon, J. R., Daniau, A. L., Field, R. D., Arneth, A., Forrest, M., Hantson, S., Kehrwald, N. M., Knorr, W., Lasslop, G., Li, F., Mangeon, S., Yue, C., Kaiser, J. W., and van der Werf, G. R.: Historic global biomass burning emissions for CMIP6 (BB4CMIP) based on merging satellite observations with proxies and fire models (1750–2015), Geoscientific Model Development, 10, 3329–3357, https://doi.org/10.5194/gmd-10-3329-2017, 2017.
1209 1210	McCormick, M. P. and Veiga, R. E.: SAGE II measurements of early Pinatubo aerosols, Geophysical Research Letters, 19, 155–158, https://doi.org/10.1029/91GL02790, 1992.
1211 1212	McCormick, M. P., Thomason, L. W., and Trepte, C. R.: Atmospheric effects of the Mt Pinatubo eruption, Nature, 373, 399–404, https://doi.org/10.1038/373399a0, 1995.
1213 1214 1215	McDermid, S. S., Montes, C., Cook, B. I., Puma, M. J., Kiang, N. Y., and Aleinov, I.: The Sensitivity of Land–Atmosphere Coupling to Modern Agriculture in the Northern Midlatitudes, Journal of Climate, 32, 465–484, https://doi.org/10.1175/JCLI-D-17-0799.1, 2019.
1216 1217 1218	McDermid, S. S., Weng, E., Puma, M., Cook, B., Hengl, T., Sanderman, J., Lannoy, G. J. M. D., and Aleinov, I.: Soil Carbon Losses Reduce Soil Moisture in Global Climate Model Simulations, Earth Interactions, 26, 195–208, https://doi.org/10.1175/El D 22 0003.1, 2022.
1219 1220 1221	McGraw, Z., DallaSanta, K., Polvani, L. M., Tsigaridis, K., Orbe, C., and Bauer, S. E.: Severe Global Cooling After Volcanic Super-Eruptions? The Answer Hinges on Unknown Aerosol Size, Journal of Climate, 37, 1449—1464, https://doi.org/10.1175/JCLI-D-23-0116.1, 2024.
1222 1223	McKee, T. B., Doesken, N. J., and Kleist, J.: THE RELATIONSHIP OF DROUGHT FREQUENCY AND DURATION TO TIME SCALES, n.d.
1224 1225 1226 1227	Miller, R. L., Cakmur, R. V., Perlwitz, J., Geogdzhayev, I. V., Ginoux, P., Koch, D., Kohfeld, K. E., Prigent, C., Ruedy, R., Schmidt, G. A., and Tegen, I.: Mineral dust aerosols in the NASA Goddard Institute for Space Sciences ModelE atmospheric general circulation model, Journal of Geophysical Research: Atmospheres, 111, https://doi.org/10.1029/2005JD005796, 2006.

- 1228 Mills, M. J., Schmidt, A., Easter, R., Solomon, S., Kinnison, D. E., Ghan, S. J., Neely III, R. R.,
- 1229 Marsh, D. R., Conley, A., Bardeen, C. G., and Gettelman, A.: Global volcanic aerosol properties
- 1230 derived from emissions, 1990–2014, using CESM1(WACCM), Journal of Geophysical Research:
- 1231 Atmospheres, 121, 2332–2348, https://doi.org/10.1002/2015JD024290, 2016.
- 1232 Milly, P. C. D. and Dunne, K. A.: Potential evapotranspiration and continental drying, Nature Clim
- 1233 Change, 6, 946–949, https://doi.org/10.1038/nclimate3046, 2016.
- 1234 Minnis, P., Harrison, E. F., Stowe, L. L., Gibson, G. G., Denn, F. M., Doelling, D. R., and Smith, W.
- 1235 L.: Radiative Climate Forcing by the Mount Pinatubo Eruption, Science, 259, 1411–1415,
- 1236 https://doi.org/10.1126/science.259.5100.1411, 1993.
- 1237 Mullapudi, A., Vibhute, A. D., Mali, S., and Patil, C. H.: A review of agricultural drought
- 1238 assessment with remote sensing data: methods, issues, challenges and opportunities, Appl
- 1239 Geomat, 15, 1–13, https://doi.org/10.1007/s12518-022-00484-6, 2023.
- 1240 Myneni, R. B., Hoffman, S., Knyazikhin, Y., Privette, J. L., Glassy, J., Tian, Y., Wang, Y., Song, X.,
- 1241 Zhang, Y., Smith, G. R., Lotsch, A., Friedl, M., Morisette, J. T., Votava, P., Nemani, R. R., and
- 1242 Running, S. W.: Global products of vegetation leaf area and fraction absorbed PAR from year one
- 1243 of MODIS data, Remote Sensing of Environment, 83, 214-231, https://doi.org/10.1016/S0034
- 1244 4257(02)00074 3, 2002.
- 1245 Narasimhan, B. and Srinivasan, R.: Development and evaluation of Soil Moisture Deficit Index
- 1246 (SMDI) and Evapotranspiration Deficit Index (ETDI) for agricultural drought monitoring,
- 1247 Agricultural and Forest Meteorology, 133, 69–88,
- 1248 https://doi.org/10.1016/j.agrformet.2005.07.012, 2005.
- 1249 Nilson, S. E. and Assmann, S. M.: The Control of Transpiration. Insights from Arabidopsis, Plant
- 1250 Physiol, 143, 19–27, https://doi.org/10.1104/pp.106.093161, 2007.
- 1251 Olesen, J. E. and Bindi, M.: Consequences of climate change for European agricultural
- 1252 productivity, land use and policy, European Journal of Agronomy, 16, 239–262,
- 1253 https://doi.org/10.1016/S1161-0301(02)00004-7, 2002.
- 1254 Paik, S., Min, S.-K., Iles, C. E., Fischer, E. M., and Schurer, A. P.: Volcanic-induced global monsoon
- 1255 drying modulated by diverse El Niño responses, Science Advances, 6, eaba1212,
- 1256 https://doi.org/10.1126/sciadv.aba1212, 2020.
- 1257 Palmer, W. C.: Keeping Track of Crop Moisture Conditions, Nationwide: The New Crop Moisture
- 1258 Index, Weatherwise, 21, 156–161, https://doi.org/10.1080/00431672.1968.9932814, 1968.
- 1259 Parker, D. E., Wilson, H., Jones, P. D., Christy, J. R., and Folland, C. K.: The Impact of Mount
- 1260 Pinatubo on World Wide Temperatures, International Journal of Climatology, 16, 487–497,
- 1261 https://doi.org/10.1002/(SICI)1097_0088(199605)16:5<487::AID_JOC39>3.0.CO;2_J, 1996.

1262 1263 1264	Pinto, J. P., Turco, R. P., and Toon, O. B.: Self limiting physical and chemical effects in volcanic eruption clouds, Journal of Geophysical Research: Atmospheres, 94, 11165–11174, https://doi.org/10.1029/JD094iD08p11165, 1989.
1265 1266 1267	Polvani, L. M., Banerjee, A., and Schmidt, A.: Northern Hemisphere continental winter warming following the 1991 Mt. Pinatubo eruption: reconciling models and observations, Atmospheric Chemistry and Physics, 19, 6351–6366, https://doi.org/10.5194/acp-19-6351-2019, 2019.
1268 1269 1270	Proctor, J., Hsiang, S., Burney, J., Burke, M., and Schlenker, W.: Estimating global agricultural effects of geoengineering using volcanic eruptions, Nature, 560, 480–483, https://doi.org/10.1038/s41586-018-0417-3, 2018.
1271 1272 1273	Ramachandran, S., Ramaswamy, V., Stenchikov, G. L., and Robock, A.: Radiative impact of the Mount Pinatubo volcanic eruption: Lower stratospheric response, Journal of Geophysical Research: Atmospheres, 105, 24409–24429, https://doi.org/10.1029/2000JD900355, 2000.
1274 1275 1276 1277	Raman, A., Verulkar, S., Mandal, N., Variar, M., Shukla, V., Dwivedi, J., Singh, B., Singh, O., Swain, P., Mall, A., Robin, S., Chandrababu, R., Jain, A., Ram, T., Hittalmani, S., Haefele, S., Piepho, HP., and Kumar, A.: Drought yield index to select high yielding rice lines under different drought stress severities, Rice, 5, 31, https://doi.org/10.1186/1939-8433-5-31, 2012.
1278 1279 1280 1281	Ramaswamy, V., Chanin, M. L., Angell, J., Barnett, J., Gaffen, D., Gelman, M., Keckhut, P., Koshelkov, Y., Labitzke, K., Lin, J. J. R., O'Neill, A., Nash, J., Randel, W., Rood, R., Shine, K., Shiotani, M., and Swinbank, R.: Stratospheric temperature trends: Observations and model simulations, Reviews of Geophysics, 39, 71–122, https://doi.org/10.1029/1999RG000065, 2001.
1282 1283 1284	Ramaswamy, V., Schwarzkopf, M. D., Randel, W. J., Santer, B. D., Soden, B. J., and Stenchikov, G. L.: Anthropogenic and Natural Influences in the Evolution of Lower Stratospheric Cooling, Science, 311, 1138–1141, https://doi.org/10.1126/science.1122587, 2006.
1285 1286	Robock, A.: Volcanic eruptions and climate, Reviews of Geophysics, 38, 191–219, https://doi.org/10.1029/1998RG000054, 2000.
1287 1288 1289	Robock, A.: Cooling following large volcanic eruptions corrected for the effect of diffuse radiation on tree rings, Geophysical Research Letters, 32, https://doi.org/10.1029/2004GL022116, 2005.
1290 1291 1292	Robock, A. and Liu, Y.: The Volcanic Signal in Goddard Institute for Space Studies Three-Dimensional Model Simulations, Journal of Climate, 7, 44–55, https://doi.org/10.1175/1520-0442(1994)007<0044:TVSIGI>2.0.CO;2, 1994.
1293 1294 1295	Rogers, H. L., Norton, W. A., Lambert, A., and Grainger, R. G.: Transport of Mt. Pinatubo aerosol by tropospheric synoptic scale and stratospheric planetary scale waves, Quarterly Journal of the Royal Meteorological Society, 124, 193—209, https://doi.org/10.1002/qj.49712454509, 1998.

1297 1298	Journal of Climate, 10, 2040 2054, https://doi.org/10.1175/1520-0442(1997)010<2040:LSMDFT>2.0.CO;2, 1997.
1299 1300	Rosenzweig, C. and Parry, M. L.: Potential impact of climate change on world food supply, Nature, 367, 133–138, https://doi.org/10.1038/367133a0, 1994.
1301 1302 1303 1304 1305	Russell, P. B., Livingston, J. M., Pueschel, R. F., Bauman, J. J., Pollack, J. B., Brooks, S. L., Hamill, P., Thomason, L. W., Stowe, L. L., Deshler, T., Dutton, E. G., and Bergstrom, R. W.: Global to microscale evolution of the Pinatubo volcanic aerosol derived from diverse measurements and analyses, Journal of Geophysical Research: Atmospheres, 101, 18745–18763, https://doi.org/10.1029/96JD01162, 1996.
1306 1307 1308 1309	Santer, B. D., Bonfils, C., Painter, J. F., Zelinka, M. D., Mears, C., Solomon, S., Schmidt, G. A., Fyfe, J. C., Cole, J. N. S., Nazarenko, L., Taylor, K. E., and Wentz, F. J.: Volcanic contribution to decadal changes in tropospheric temperature, Nature Geosci, 7, 185–189, https://doi.org/10.1038/ngeo2098, 2014.
1310 1311 1312	Sato, M., Hansen, J. E., McCormick, M. P., and Pollack, J. B.: Stratospheric aerosol optical depths, 1850–1990, Journal of Geophysical Research: Atmospheres, 98, 22987–22994, https://doi.org/10.1029/93JD02553, 1993.
1313 1314	Scheff, J. and Frierson, D. M. W.: Terrestrial Aridity and Its Response to Greenhouse Warming across CMIPS Climate Models, https://doi.org/10.1175/JCLI-D-14-00480.1, 2015.
1315 1316	Self, S., Zhao, JX., Holasek, R. E., Torres, R. C., and King, A. J.: The Atmospheric Impact of the 1991 Mount Pinatubo Eruption, 1993.
1317 1318 1319	Seneviratne, S. I., Corti, T., Davin, E. L., Hirschi, M., Jaeger, E. B., Lehner, I., Orlowsky, B., and Teuling, A. J.: Investigating soil moisture—climate interactions in a changing climate: A review, Earth Science Reviews, 99, 125–161, https://doi.org/10.1016/j.earscirev.2010.02.004, 2010.
1320 1321 1322 1323	Sheng, J. X., Weisenstein, D. K., Luo, B. P., Rozanov, E., Arfeuille, F., and Peter, T.: A perturbed parameter model ensemble to investigate Mt. Pinatubo's 1991 initial sulfur mass emission, Atmospheric Chemistry and Physics, 15, 11501–11512, https://doi.org/10.5194/acp-15-11501-2015, 2015a.
1324 1325 1326 1327	Sheng, JX., Weisenstein, D. K., Luo, BP., Rozanov, E., Stenke, A., Anet, J., Bingemer, H., and Peter, T.: Global atmospheric sulfur budget under volcanically quiescent conditions: Aerosol-chemistry climate model predictions and validation, Journal of Geophysical Research: Atmospheres, 120, 256–276, https://doi.org/10.1002/2014JD021985, 2015b.

Rosenzweig, C. and Abramopoulos, F.: Land Surface Model Development for the GISS GCM,

1296

1328 1329

Shindell, D. T.: Climate and ozone response to increased stratospheric water vapor, Geophysical

Research Letters, 28, 1551–1554, https://doi.org/10.1029/1999GL011197, 2001.

1330 Shindell, D. T., Faluvegi, G., and Bell, N.: Preindustrial to present day radiative forcing by 1331 tropospheric ozone from improved simulations with the GISS chemistry climate GCM, 1332 Atmospheric Chemistry and Physics, 3, 1675-1702, https://doi.org/10.5194/acp-3-1675-2003, 1333 2003. 1334 Shindell, D. T., Faluvegi, G., Unger, N., Aguilar, E., Schmidt, G. A., Koch, D. M., Bauer, S. E., and 1335 Miller, R. L.: Simulations of preindustrial, present-day, and 2100 conditions in the NASA GISS composition and climate model G-PUCCINI, Atmospheric Chemistry and Physics, 6, 4427–4459, 1336 1337 https://doi.org/10.5194/acp-6-4427-2006, 2006. 1338 Sigl, M., Winstrup, M., McConnell, J. R., Welten, K. C., Plunkett, G., Ludlow, F., Büntgen, U., 1339 Caffee, M., Chellman, N., Dahl Jensen, D., Fischer, H., Kipfstuhl, S., Kostick, C., Maselli, O. J., 1340 Mekhaldi, F., Mulvaney, R., Muscheler, R., Pasteris, D. R., Pilcher, J. R., Salzer, M., Schüpbach, S., 1341 Steffensen, J. P., Vinther, B. M., and Woodruff, T. E.: Timing and climate forcing of volcanic eruptions for the past 2,500 years, Nature, 523, 543-549, https://doi.org/10.1038/nature14565, 1342 1343 2015. Simard, M., Pinto, N., Fisher, J. B., and Baccini, A.: Mapping forest canopy height globally with 1344 1345 spaceborne lidar, Journal of Geophysical Research: Biogeosciences, 116, 1346 https://doi.org/10.1029/2011JG001708, 2011. 1347 Singh, R., Tsigaridis, K., LeGrande, A. N., Ludlow, F., and Manning, J. G.: Investigating hydroclimatic impacts of the 168–158 BCE volcanic quartet and their relevance to the 1348 1349 Nile River basin and Egyptian history, Climate of the Past, 19, 249-275, 1350 https://doi.org/10.5194/cp 19 249 2023, 2023. 1351 Soden, B. J., Wetherald, R. T., Stenchikov, G. L., and Robock, A.: Global Cooling After the Eruption 1352 of Mount Pinatubo: A Test of Climate Feedback by Water Vapor, Science, 296, 727-730, 1353 https://doi.org/10.1126/science.296.5568.727, 2002. 1354 Stenchikov, G. L., Kirchner, I., Robock, A., Graf, H. F., Antuña, J. C., Grainger, R. G., Lambert, A., 1355 and Thomason, L.: Radiative forcing from the 1991 Mount Pinatubo volcanic eruption, Journal 1356 of Geophysical Research: Atmospheres, 103, 13837-13857, 1357 https://doi.org/10.1029/98JD00693, 1998. 1358 Tejedor, E., Steiger, N. J., Smerdon, J. E., Serrano-Notivoli, R., and Vuille, M.: Global hydroclimatic 1359 response to tropical volcanic eruptions over the last millennium, Proceedings of the National 1360 Academy of Sciences, 118, e2019145118, https://doi.org/10.1073/pnas.2019145118, 2021. 1361 Thornthwaite, C. W.: An Approach toward a Rational Classification of Climate, Geographical 1362 Review, 38, 55-94, https://doi.org/10.2307/210739, 1948.

Timmreck, C., Graf, H.-F., and Feichter, J.: Simulation of Mt. Pinatubo Volcanic Aerosol with the

Hamburg Climate Model ECHAM4, Theor Appl Climatol, 62, 85-108,

https://doi.org/10.1007/s007040050076, 1999.

1363

1364

1366	Toohey, M., Krüger, K., Sigl, M., Stordal, F., and Svensen, H.: Climatic and societal impacts of a
1367	volcanic double event at the dawn of the Middle Ages, Climatic Change, 136, 401–412,
1368	https://doi.org/10.1007/s10584-016-1648-7, 2016.
1369	Toohey, M., Krüger, K., Schmidt, H., Timmreck, C., Sigl, M., Stoffel, M., and Wilson, R.:
1370	Disproportionately strong climate forcing from extratropical explosive volcanic eruptions,
1871	Nature Geosci, 12, 100–107, https://doi.org/10.1038/s41561-018-0286-2, 2019.
15/1	Nature deose, 12, 100–107, https://doi.org/10.1036/341301-016-0260-2, 2013.
1372	Trenberth, K. E. and Dai, A.: Effects of Mount Pinatubo volcanic eruption on the hydrological
1373	cycle as an analog of geoengineering, Geophysical Research Letters, 34,
1374	https://doi.org/10.1029/2007GL030524. 2007.
15/4	https://doi.org/10.1025/2007GL050524, 2007.
1375	Trenberth, K. E. and Stepaniak, D. P.: The flow of energy through the earth's climate system,
1376	Quarterly Journal of the Royal Meteorological Society, 130, 2677–2701,
1377	https://doi.org/10.1256/qj.04.83, 2004.
15//	11ttps://doi.org/10.1250/qj.04.65, 2004.
1378	Trenberth, K. E., Fasullo, J. T., and Kiehl, J.: Earth's Global Energy Budget, Bulletin of the
1379	American Meteorological Society, 90, 311–324, https://doi.org/10.1175/2008BAMS2634.1,
1380	2009.
1580	2009.
1381	Trepte, C. R., Veiga, R. E., and McCormick, M. P.: The poleward dispersal of Mount Pinatubo
1382	volcanic aerosol, Journal of Geophysical Research: Atmospheres, 98, 18563–18573,
1383	https://doi.org/10.1029/93JD01362, 1993.
1503	Https://doi.org/10.1029/93/D01302, 1993.
1384	Vehkamäki, H., Kulmala, M., Napari, I., Lehtinen, K. E. J., Timmreck, C., Noppel, M., and
1385	Laaksonen, A.: An improved parameterization for sulfuric acid—water nucleation rates for
1386	tropospheric and stratospheric conditions, Journal of Geophysical Research: Atmospheres, 107,
1387	AAC 3 1 AAC 3 10, https://doi.org/10.1029/2002JD002184, 2002.
1507	AAC 5 1 AAC 5 10, https://doi.org/10.1025/200230002164, 2002.
1388	Wada, Y., Wisser, D., Eisner, S., Flörke, M., Gerten, D., Haddeland, I., Hanasaki, N., Masaki, Y.,
1389	Portmann, F. T., Stacke, T., Tessler, Z., and Schewe, J.: Multimodel projections and uncertainties
1390	of irrigation water demand under climate change, Geophysical Research Letters, 40, 4626–4632,
1391	
1991	https://doi.org/10.1002/grl.50686, 2013.
1392	Weng, E., Aleinov, I., Singh, R., Puma, M. J., McDermid, S. S., Kiang, N. Y., Kelley, M., Wilcox, K.,
1393	Dybzinski, R., Farrior, C. E., Pacala, S. W., and Cook, B. I.: Modeling demographic-driven
1394	
	vegetation dynamics and ecosystem biogeochemical cycling in NASA GISS's Earth system
1395	model (ModelE BiomeE v.1.0), Geoscientific Model Development Discussions, 1–60,
1396	https://doi.org/10.5194/gmd 2022 72, 2022.
1397	van der Werf, G. R., Randerson, J. T., Giglio, L., van Leeuwen, T. T., Chen, Y., Rogers, B. M., Mu,
1398	M., van Marle, M. J. E., Morton, D. C., Collatz, G. J., Yokelson, R. J., and Kasibhatla, P. S.: Global
1399	fire emissions estimates during 1997–2016, Earth System Science Data, 9, 697–720,
1400	https://doi.org/10.5194/essd-9-697-2017, 2017.

1401 1402 1403	Wisser, D., Fekete, B. M., Vörösmarty, C. J., and Schumann, A. H.: Reconstructing 20th century global hydrography: a contribution to the Global Terrestrial Network Hydrology (GTN H), Hydrology and Earth System Sciences, 14, 1–24, https://doi.org/10.5194/hess 14 1 2010, 2010.
1404 1405 1406	Zambri, B. and Robock, A.: Winter warming and summer monsoon reduction after volcanic eruptions in Coupled Model Intercomparison Project 5 (CMIP5) simulations, Geophysical Research Letters, 43, 10,920-10,928, https://doi.org/10.1002/2016GL070460, 2016.
1407 1408 1409 1410	Zambri, B., LeGrande, A. N., Robock, A., and Slawinska, J.: Northern Hemisphere winter warming and summer monsoon reduction after volcanic eruptions over the last millennium, Journal of Geophysical Research: Atmospheres, 122, 7971—7989, https://doi.org/10.1002/2017JD026728, 2017.
1411 1412 1413	Zhao, J., Turco, R. P., and Toon, O. B.: A model simulation of Pinatubo volcanic aerosols in the stratosphere, Journal of Geophysical Research: Atmospheres, 100, 7315–7328, https://doi.org/10.1029/94JD03325, 1995.
1414	±
1415 1416 1417	Aquila, V., Oman, L. D., Stolarski, R. S., Colarco, P. R., and Newman, P. A.: Dispersion of the volcanic sulfate cloud from a Mount Pinatubo—like eruption, Journal of Geophysical Research: Atmospheres, 117, https://doi.org/10.1029/2011JD016968, 2012.
1418 1419 1420	Barnes, E. A., Solomon, S., and Polvani, L. M.: Robust Wind and Precipitation Responses to the Mount Pinatubo Eruption, as Simulated in the CMIP5 Models, Journal of Climate, 29, 4763–4778, https://doi.org/10.1175/JCLI-D-15-0658.1, 2016.
1421 1422 1423	Barnes, J. E. and Hofmann, D. J.: Lidar measurements of stratospheric aerosol over Mauna Loa Observatory, Geophysical Research Letters, 24, 1923–1926, https://doi.org/10.1029/97GL01943, 1997.
1424 1425 1426 1427	Bauer, S. E., Wright, D. L., Koch, D., Lewis, E. R., McGraw, R., Chang, LS., Schwartz, S. E., and Ruedy, R.: MATRIX (Multiconfiguration Aerosol TRacker of mlXing state): an aerosol microphysical module for global atmospheric models, Atmospheric Chemistry and Physics, 8, 6003–6035, https://doi.org/10.5194/acp-8-6003-2008, 2008.
1428 1429 1430 1431	Bauer, S. E., Ault, A., and Prather, K. A.: Evaluation of aerosol mixing state classes in the GISS modelE-MATRIX climate model using single-particle mass spectrometry measurements, Journal of Geophysical Research: Atmospheres, 118, 9834–9844, https://doi.org/10.1002/jgrd.50700, 2013.
1432 1433 1434 1435	Bauer, S. E., Tsigaridis, K., Faluvegi, G., Kelley, M., Lo, K. K., Miller, R. L., Nazarenko, L., Schmidt, G. A., and Wu, J.: Historical (1850–2014) Aerosol Evolution and Role on Climate Forcing Using the GISS ModelE2.1 Contribution to CMIP6, Journal of Advances in Modeling Earth Systems, 12, e2019MS001978, https://doi.org/10.1029/2019MS001978, 2020.

- 1436 Bluth, G. J. S., Doiron, S. D., Schnetzler, C. C., Krueger, A. J., and Walter, L. S.: Global tracking of
- 1437 the SO2 clouds from the June, 1991 Mount Pinatubo eruptions, Geophysical Research Letters,
- 1438 <u>19, 151–154, https://doi.org/10.1029/91GL02792, 1992.</u>
- 1439 Briffa, K. R., Jones, P. D., Schweingruber, F. H., and Osborn, T. J.: Influence of volcanic eruptions
- 1440 on Northern Hemisphere summer temperature over the past 600 years, Nature, 393, 450–455,
- 1441 https://doi.org/10.1038/30943, 1998.
- 1442 Brown, H. Y., Wagman, B., Bull, D., Peterson, K., Hillman, B., Liu, X., Ke, Z., and Lin, L.: Validating
- 1443 a microphysical prognostic stratospheric aerosol implementation in E3SMv2 using observations
- 1444 after the Mount Pinatubo eruption, Geoscientific Model Development, 17, 5087–5121,
- 1445 https://doi.org/10.5194/gmd-17-5087-2024, 2024.
- 1446 Carn, S. A., Clarisse, L., and Prata, A. J.: Multi-decadal satellite measurements of global volcanic
- degassing, Journal of Volcanology and Geothermal Research, 311, 99–134,
- 1448 <u>https://doi.org/10.1016/j.jvolgeores.2016.01.002, 2016.</u>
- 1449 Chen, D.-X. and Coughenour, M. B.: Photosynthesis, transpiration, and primary productivity:
- 1450 Scaling up from leaves to canopies and regions using process models and remotely sensed data,
- 1451 Global Biogeochemical Cycles, 18, https://doi.org/10.1029/2002GB001979, 2004.
- 1452 Cheng, W., MacMartin, D. G., Dagon, K., Kravitz, B., Tilmes, S., Richter, J. H., Mills, M. J., and
- 1453 Simpson, I. R.: Soil Moisture and Other Hydrological Changes in a Stratospheric Aerosol
- 1454 Geoengineering Large Ensemble, Journal of Geophysical Research: Atmospheres, 124, 12773–
- 1455 12793, https://doi.org/10.1029/2018JD030237, 2019.
- 1456 <u>Colose, C. M., LeGrande, A. N., and Vuille, M.: Hemispherically asymmetric volcanic forcing of</u>
- tropical hydroclimate during the last millennium, Earth System Dynamics, 7, 681–696,
- 1458 <u>https://doi.org/10.5194/esd-7-681-2016, 2016.</u>
- 1459 Cook, B. I., McDermid, S. S., Puma, M. J., Williams, A. P., Seager, R., Kelley, M., Nazarenko, L., and
- 1460 Aleinov, I.: Divergent Regional Climate Consequences of Maintaining Current Irrigation Rates in
- the 21st Century, Journal of Geophysical Research: Atmospheres, 125, e2019JD031814,
- 1462 <u>https://doi.org/10.1029/2019JD031814, 2020.</u>
- 1463 Denissen, J. M. C., Teuling, A. J., Pitman, A. J., Koirala, S., Migliavacca, M., Li, W., Reichstein, M.,
- 1464 Winkler, A. J., Zhan, C., and Orth, R.: Widespread shift from ecosystem energy to water
- 1465 limitation with climate change, Nat. Clim. Chang., 12, 677–684, https://doi.org/10.1038/s41558-
- 1466 <u>022-01403-8, 2022.</u>
- 1467 Deshler, T., Hervig, M. E., Hofmann, D. J., Rosen, J. M., and Liley, J. B.: Thirty years of in situ
- 1468 <u>stratospheric aerosol size distribution measurements from Laramie, Wyoming (41°N), using</u>
- 1469 balloon-borne instruments, Journal of Geophysical Research: Atmospheres, 108,
- 1470 https://doi.org/10.1029/2002JD002514, 2003.

- 1471 <u>Dhomse, S. S., Emmerson, K. M., Mann, G. W., Bellouin, N., Carslaw, K. S., Chipperfield, M. P.,</u>
- 1472 Hommel, R., Abraham, N. L., Telford, P., Braesicke, P., Dalvi, M., Johnson, C. E., O'Connor, F.,
- 1473 Morgenstern, O., Pyle, J. A., Deshler, T., Zawodny, J. M., and Thomason, L. W.: Aerosol
- 1474 <u>microphysics simulations of the Mt.~Pinatubo eruption with the UM-UKCA composition-climate</u>
- 1475 model, Atmospheric Chemistry and Physics, 14, 11221–11246, https://doi.org/10.5194/acp-14-
- 1476 11221-2014, 2014.
- 1477 van Dijk, E., Mørkestøl Gundersen, I., de Bode, A., Høeg, H., Loftsgarden, K., Iversen, F.,
- 1478 <u>Timmreck, C., Jungclaus, J., and Krüger, K.: Climatic and societal impacts in Scandinavia following</u>
- 1479 <u>the 536 and 540 CE volcanic double event, Climate of the Past, 19, 357–398,</u>
- 1480 <u>https://doi.org/10.5194/cp-19-357-2023, 2023.</u>
- 1481 <u>Dirmeyer, P. A., Gao, X., Zhao, M., Guo, Z., Oki, T., and Hanasaki, N.: GSWP-2: Multimodel</u>
- 1482 Analysis and Implications for Our Perception of the Land Surface,
- 1483 <u>https://doi.org/10.1175/BAMS-87-10-1381, 2006.</u>
- 1484 Dong, B. and Dai, A.: The uncertainties and causes of the recent changes in global
- 1485 <u>evapotranspiration from 1982 to 2010, Clim Dyn, 49, 279–296, https://doi.org/10.1007/s00382-</u>
- 1486 <u>016-3342-x, 2017.</u>
- 1487 <u>Dutton, E. G. and Christy, J. R.: Solar radiative forcing at selected locations and evidence for</u>
- 1488 global lower tropospheric cooling following the eruptions of El Chichón and Pinatubo,
- 1489 <u>Geophysical Research Letters, 19, 2313–2316, https://doi.org/10.1029/92GL02495, 1992.</u>
- 1490 English, J. M., Toon, O. B., and Mills, M. J.: Microphysical simulations of large volcanic eruptions:
- 1491 <u>Pinatubo and Toba, Journal of Geophysical Research: Atmospheres, 118, 1880–1895,</u>
- 1492 https://doi.org/10.1002/jgrd.50196, 2013.
- 1493 Farquhar, G. D. and Roderick, M. L.: Pinatubo, Diffuse Light, and the Carbon Cycle, Science, 299,
- 1494 1997–1998, https://doi.org/10.1126/science.1080681, 2003.
- 1495 <u>Frölicher, T. L., Joos, F., and Raible, C. C.: Sensitivity of atmospheric CO₂ and climate to explosive</u>
- 1496 volcanic eruptions, Biogeosciences, 8, 2317–2339, https://doi.org/10.5194/bg-8-2317-2011,
- 1497 <u>2011.</u>
- 1498 Gao, C. Y., Naik, V., Horowitz, L. W., Ginoux, P., Paulot, F., Dunne, J., Mills, M., Aquila, V., and
- 1499 Colarco, P.: Volcanic Drivers of Stratospheric Sulfur in GFDL ESM4, Journal of Advances in
- 1500 Modeling Earth Systems, 15, e2022MS003532, https://doi.org/10.1029/2022MS003532, 2023.
- 1501 Gao, F., Morisette, J. T., Wolfe, R. E., Ederer, G., Pedelty, J., Masuoka, E., Myneni, R., Tan, B., and
- 1502 <u>Nightingale, J.: An Algorithm to Produce Temporally and Spatially Continuous MODIS-LAI Time</u>
- 1503 <u>Series, IEEE Geoscience and Remote Sensing Letters, 5, 60–64,</u>
- 1504 https://doi.org/10.1109/LGRS.2007.907971, 2008.

- 1505 Gery, M. W., Whitten, G. Z., Killus, J. P., and Dodge, M. C.: A photochemical kinetics mechanism
- 1506 for urban and regional scale computer modeling, Journal of Geophysical Research:
- 1507 <u>Atmospheres, 94, 12925–12956, https://doi.org/10.1029/JD094iD10p12925, 1989.</u>
- 1508 Gu, G. and Adler, R. F.: Large-scale, inter-annual relations among surface temperature, water
- 1509 vapour and precipitation with and without ENSO and volcano forcings, International Journal of
- 1510 Climatology, 32, 1782–1791, https://doi.org/10.1002/joc.2393, 2012.
- 1511 Gu, G., Adler, R. F., Huffman, G. J., and Curtis, S.: Tropical Rainfall Variability on Interannual-to-
- 1512 Interdecadal and Longer Time Scales Derived from the GPCP Monthly Product, Journal of
- 1513 Climate, 20, 4033–4046, https://doi.org/10.1175/JCLI4227.1, 2007.
- 1514 Gu, L., Baldocchi, D., Verma, S. B., Black, T. A., Vesala, T., Falge, E. M., and Dowty, P. R.:
- 1515 Advantages of diffuse radiation for terrestrial ecosystem productivity, Journal of Geophysical
- 1516 Research: Atmospheres, 107, ACL 2-1-ACL 2-23, https://doi.org/10.1029/2001JD001242, 2002.
- 1517 Gu, L., Baldocchi, D. D., Wofsy, S. C., Munger, J. W., Michalsky, J. J., Urbanski, S. P., and Boden, T.
- 1518 A.: Response of a Deciduous Forest to the Mount Pinatubo Eruption: Enhanced Photosynthesis,
- 1519 <u>Science, 299, 2035–2038, https://doi.org/10.1126/science.1078366, 2003.</u>
- 1520 Hane, D. C. and Pumphrey, F. V.: Yield-evapotranspiration relationships and seasonal crop
- coefficients for frequently irrigated potatoes, American Potato Journal, 61, 661–668,
- 1522 https://doi.org/10.1007/BF02852929, 1984.
- 1523 <u>Hansen, J., Lacis, A., Ruedy, R., and Sato, M.: Potential climate impact of Mount Pinatubo</u>
- eruption, Geophysical Research Letters, 19, 215–218, https://doi.org/10.1029/91GL02788,
- **1525 1992**.

- 1526 Hansen, J., Sato, M., Ruedy, R., Lacis, A., Asamoah, K., Borenstein, S., Brown, E., Cairns, B., Caliri,
- 1527 G., Campbell, M., Curran, B., de Castro, S., Druyan, L., Fox, M., Johnson, C., Lerner, J.,
- 1528 McCormick, M. P., Miller, R., Minnis, P., Morrison, A., Pandolfo, L., Ramberrann, I., Zaucker, F.,
- 1529 Robinson, M., Russell, P., Shah, K., Stone, P., Tegen, I., Thomason, L., Wilder, J., and Wilson, H.: A
- 1530 <u>Pinatubo Climate Modeling Investigation, in: The Mount Pinatubo Eruption, Berlin, Heidelberg,</u>
- 1531 <u>233–272, https://doi.org/10.1007/978-3-642-61173-5 20, 1996.</u>
- 1532 Hansen, J. E., Lacis, A. A., Lee, P., and Wang, W.-C.: Climatic Effects of Atmospheric Aerosols,
- <u>Annals of the New York Academy of Sciences, 338, 575–587, https://doi.org/10.1111/j.1749-</u>
- 1534 6632.1980.tb17151.x, 1980.
- 1535 Hao, Z., Xiong, D., Zheng, J., Yang, L. E., and Ge, Q.: Volcanic eruptions, successive poor harvests
- and social resilience over southwest China during the 18–19th century, Environ. Res. Lett., 15,
- 1537 <u>105011, https://doi.org/10.1088/1748-9326/abb159, 2020.</u>
- 1538 Hitchman, M. H., M. McKay, C. R. Trepte, A climatology of stratospheric aerosol, J. Geophys.
- 1539 Res., 99, 20689–20700, 1994

- 1541 Hoesly, R. M., Smith, S. J., Feng, L., Klimont, Z., Janssens-Maenhout, G., Pitkanen, T., Seibert, J. J.,
- 1542 <u>Vu, L., Andres, R. J., Bolt, R. M., Bond, T. C., Dawidowski, L., Kholod, N., Kurokawa, J., Li, M., Liu,</u>
- 1543 <u>L., Lu, Z., Moura, M. C. P., O'Rourke, P. R., and Zhang, Q.: Historical (1750–2014) anthropogenic</u>
- 1544 emissions of reactive gases and aerosols from the Community Emissions Data System (CEDS),
- 1545 Geoscientific Model Development, 11, 369–408, https://doi.org/10.5194/gmd-11-369-2018,
- **1546 2018**.
- 1547 Huhtamaa, H. and Helama, S.: Distant impact: tropical volcanic eruptions and climate-driven
- 1548 agricultural crises in seventeenth-century Ostrobothnia, Finland, Journal of Historical
- 1549 <u>Geography, 57, 40–51, https://doi.org/10.1016/j.jhg.2017.05.011, 2017.</u>
- 1550 <u>lles, C. E., Hegerl, G. C., Schurer, A. P., and Zhang, X.: The effect of volcanic eruptions on global</u>
- precipitation, Journal of Geophysical Research: Atmospheres, 118, 8770–8786,
- 1552 <u>https://doi.org/10.1002/jgrd.50678, 2013.</u>
- 1553 <u>Ito, G., Romanou, A., Kiang, N. Y., Faluvegi, G., Aleinov, I., Ruedy, R., Russell, G., Lerner, P., Kelley, </u>
- 1554 M., and Lo, K.: Global Carbon Cycle and Climate Feedbacks in the NASA GISS ModelE2.1, Journal
- of Advances in Modeling Earth Systems, 12, e2019MS002030,
- 1556 https://doi.org/10.1029/2019MS002030, 2020.
- 1557 Jones, C. D. and Cox, P. M.: Modeling the volcanic signal in the atmospheric CO2 record, Global
- 1558 Biogeochemical Cycles, 15, 453–465, https://doi.org/10.1029/2000GB001281, 2001.
- 1559 Joseph, R. and Zeng, N.: Seasonally Modulated Tropical Drought Induced by Volcanic Aerosol,
- 1560 Journal of Climate, 24, 2045–2060, https://doi.org/10.1175/2009JCLI3170.1, 2011.
- 1561 Kandlbauer, J., Hopcroft, P. O., Valdes, P. J., and Sparks, R. S. J.: Climate and carbon cycle
- 1562 response to the 1815 Tambora volcanic eruption, Journal of Geophysical Research:
- 1563 Atmospheres, 118, 12,497-12,507, https://doi.org/10.1002/2013JD019767, 2013.
- 1564 Kelley, M., Schmidt, G. A., Nazarenko, L. S., Bauer, S. E., Ruedy, R., Russell, G. L., Ackerman, A. S.,
- Aleinov, I., Bauer, M., Bleck, R., Canuto, V., Cesana, G., Cheng, Y., Clune, T. L., Cook, B. I., Cruz, C.
- 1566 A., Del Genio, A. D., Elsaesser, G. S., Faluvegi, G., Kiang, N. Y., Kim, D., Lacis, A. A., Leboissetier,
- 1567 A., LeGrande, A. N., Lo, K. K., Marshall, J., Matthews, E. E., McDermid, S., Mezuman, K., Miller, R.
- 1568 L., Murray, L. T., Oinas, V., Orbe, C., García-Pando, C. P., Perlwitz, J. P., Puma, M. J., Rind, D.,
- Romanou, A., Shindell, D. T., Sun, S., Tausnev, N., Tsigaridis, K., Tselioudis, G., Weng, E., Wu, J.,
- and Yao, M.-S.: GISS-E2.1: Configurations and Climatology, Journal of Advances in Modeling
- 1571 <u>Earth Systems, 12, e2019MS002025, https://doi.org/10.1029/2019MS002025, 2020.</u>
- 1572 Keshavarz, M. R., Vazifedoust, M., and Alizadeh, A.: Drought monitoring using a Soil Wetness
- 1573 Deficit Index (SWDI) derived from MODIS satellite data, Agricultural Water Management, 132,
- 1574 37–45, https://doi.org/10.1016/j.agwat.2013.10.004, 2014.

- 1575 <u>Kiehl, J. T. and Trenberth, K. E.: Earth's Annual Global Mean Energy Budget, Bulletin of the</u>
- 1576 <u>American Meteorological Society, 78, 197–208, https://doi.org/10.1175/1520-</u>
- 1577 <u>0477(1997)078<0197:EAGMEB>2.0.CO;2, 1997.</u>
- 1578 Kim, Y., Moorcroft, P. R., Aleinov, I., Puma, M. J., and Kiang, N. Y.: Variability of phenology and
- 1579 fluxes of water and carbon with observed and simulated soil moisture in the Ent Terrestrial
- 1580 <u>Biosphere Model (Ent TBM version 1.0.1.0.0), Geoscientific Model Development, 8, 3837–3865,</u>
- 1581 <u>https://doi.org/10.5194/gmd-8-3837-2015, 2015.</u>
- 1582 Kinne, S., Toon, O. B., and Prather, M. J.: Buffering of stratospheric circulation by changing
- 1583 <u>amounts of tropical ozone a Pinatubo case study, Geophysical Research Letters (American</u>
- 1584 <u>Geophysical Union); (United States), 19:19, https://doi.org/10.1029/92GL01937, 1992.</u>
- 1585 Kirchner, I., Stenchikov, G. L., Graf, H.-F., Robock, A., and Antuña, J. C.: Climate model simulation
- 1586 of winter warming and summer cooling following the 1991 Mount Pinatubo volcanic eruption,
- 1587 <u>Journal of Geophysical Research: Atmospheres, 104, 19039–19055,</u>
- 1588 <u>https://doi.org/10.1029/1999JD900213, 1999.</u>
- 1589 <u>Krakauer, N. Y. and Randerson, J. T.: Do volcanic eruptions enhance or diminish net primary</u>
- 1590 <u>production? Evidence from tree rings, Global Biogeochemical Cycles, 17,</u>
- 1591 <u>https://doi.org/10.1029/2003GB002076, 2003.</u>
- 1592 Kremser, S., Thomason, L. W., von Hobe, M., Hermann, M., Deshler, T., Timmreck, C., Toohey, M.,
- 1593 <u>Stenke, A., Schwarz, J. P., Weigel, R., Fueglistaler, S., Prata, F. J., Vernier, J.-P., Schlager, H., Barnes,</u>
- 1594 J. E., Antuña-Marrero, J.-C., Fairlie, D., Palm, M., Mahieu, E., Notholt, J., Rex, M., Bingen, C.,
- 1595 <u>Vanhellemont, F., Bourassa, A., Plane, J. M. C., Klocke, D., Carn, S. A., Clarisse, L., Trickl, T., Neely,</u>
- 1596 R., James, A. D., Rieger, L., Wilson, J. C., and Meland, B.: Stratospheric aerosol—Observations,
- processes, and impact on climate, Reviews of Geophysics, 54, 278–335,
- 1598 https://doi.org/10.1002/2015RG000511, 2016.
- Labitzke, K. and McCormick, M. P.: Stratospheric temperature increases due to Pinatubo
- aerosols, Geophysical Research Letters, 19, 207–210, https://doi.org/10.1029/91GL02940,
- 1601 <u>1992.</u>
- Lacis, A.: Volcanic aerosol radiative properties, PAGES Mag, 23, 50–51,
- 1603 <u>https://doi.org/10.22498/pages.23.2.50, 2015.</u>
- Lacis, A., Hansen, J., and Sato, M.: Climate forcing by stratospheric aerosols, Geophysical
- 1605 Research Letters, 19, 1607–1610, https://doi.org/10.1029/92GL01620, 1992.
- 1606 Lacis, A. A. and Hansen, J.: A Parameterization for the Absorption of Solar Radiation in the
- 1607 <u>Earth's Atmosphere, Journal of the Atmospheric Sciences, 31, 118–133,</u>
- 1608 https://doi.org/10.1175/1520-0469(1974)031<0118:APFTAO>2.0.CO;2, 1974.

- 1609 <u>Lawrence, D. M., Thornton, P. E., Oleson, K. W., and Bonan, G. B.: The Partitioning of</u>
- 1610 <u>Evapotranspiration into Transpiration, Soil Evaporation, and Canopy Evaporation in a GCM:</u>
- 1611 <u>Impacts on Land–Atmosphere Interaction, https://doi.org/10.1175/JHM596.1, 2007.</u>
- 1612 LeGrande, A. N., Tsigaridis, K., and Bauer, S. E.: Role of atmospheric chemistry in the climate
- impacts of stratospheric volcanic injections, Nature Geosci, 9, 652–655,
- 1614 https://doi.org/10.1038/ngeo2771, 2016.
- Liu, F., Chai, J., Wang, B., Liu, J., Zhang, X., and Wang, Z.: Global monsoon precipitation
- responses to large volcanic eruptions, Sci Rep, 6, 24331, https://doi.org/10.1038/srep24331,
- 1617 **2016**.
- 1618 Lobell, D. B. and Field, C. B.: Global scale climate—crop yield relationships and the impacts of
- 1619 recent warming, Environ. Res. Lett., 2, 014002, https://doi.org/10.1088/1748-9326/2/1/014002,
- 1620 <u>2007</u>.
- Lucht, W., Prentice, I. C., Myneni, R. B., Sitch, S., Friedlingstein, P., Cramer, W., Bousquet, P.,
- 1622 Buermann, W., and Smith, B.: Climatic Control of the High-Latitude Vegetation Greening Trend
- 1623 and Pinatubo Effect, Science, 296, 1687–1689, https://doi.org/10.1126/science.1071828, 2002.
- Manning, J. G., Ludlow, F., Stine, A. R., Boos, W. R., Sigl, M., and Marlon, J. R.: Volcanic
- suppression of Nile summer flooding triggers revolt and constrains interstate conflict in ancient
- 1626 Egypt, Nat Commun, 8, 900, https://doi.org/10.1038/s41467-017-00957-y, 2017.
- van Marle, M. J. E., Kloster, S., Magi, B. I., Marlon, J. R., Daniau, A.-L., Field, R. D., Arneth, A.,
- 1628 Forrest, M., Hantson, S., Kehrwald, N. M., Knorr, W., Lasslop, G., Li, F., Mangeon, S., Yue, C.,
- 1629 Kaiser, J. W., and van der Werf, G. R.: Historic global biomass burning emissions for CMIP6
- (BB4CMIP) based on merging satellite observations with proxies and fire models (1750–2015),
- 1631 Geoscientific Model Development, 10, 3329–3357, https://doi.org/10.5194/gmd-10-3329-2017,
- 1632 <u>2017.</u>
- 1633 Marshall, L. R., Maters, E. C., Schmidt, A., Timmreck, C., Robock, A., and Toohey, M.: Volcanic
- 1634 <u>effects on climate: recent advances and future avenues, Bull Volcanol, 84, 54,</u>
- 1635 https://doi.org/10.1007/s00445-022-01559-3, 2022.
- 1636 McDermid, S. S., Montes, C., Cook, B. I., Puma, M. J., Kiang, N. Y., and Aleinov, I.: The Sensitivity
- 1637 <u>of Land–Atmosphere Coupling to Modern Agriculture in the Northern Midlatitudes, Journal of</u>
- 1638 <u>Climate, 32, 465–484, https://doi.org/10.1175/JCLI-D-17-0799.1, 2019.</u>
- 1639 McDermid, S. S., Weng, E., Puma, M., Cook, B., Hengl, T., Sanderman, J., Lannoy, G. J. M. D., and
- Aleinov, I.: Soil Carbon Losses Reduce Soil Moisture in Global Climate Model Simulations, Earth
- 1641 <u>Interactions, 26, 195–208, https://doi.org/10.1175/EI-D-22-0003.1, 2022.</u>
- 1642 McGraw, Z. and Polvani, L. M.: How Volcanic Aerosols Globally Inhibit Precipitation, Geophysical
- 1643 Research Letters, 51, e2023GL107930, https://doi.org/10.1029/2023GL107930, 2024.

- 1644 McKee, T. B., Doesken, N. J., and Kleist, J.: THE RELATIONSHIP OF DROUGHT FREQUENCY AND
- 1645 DURATION TO TIME SCALES, n.d.
- Miller, R. L., Cakmur, R. V., Perlwitz, J., Geogdzhayev, I. V., Ginoux, P., Koch, D., Kohfeld, K. E.,
- 1647 Prigent, C., Ruedy, R., Schmidt, G. A., and Tegen, I.: Mineral dust aerosols in the NASA Goddard
- 1648 <u>Institute for Space Sciences ModelE atmospheric general circulation model, Journal of</u>
- 1649 <u>Geophysical Research: Atmospheres, 111, https://doi.org/10.1029/2005JD005796, 2006.</u>
- Miller, R. L., Schmidt, G. A., Nazarenko, L. S., Bauer, S. E., Kelley, M., Ruedy, R., Russell, G. L.,
- 1651 Ackerman, A. S., Aleinov, I., Bauer, M., Bleck, R., Canuto, V., Cesana, G., Cheng, Y., Clune, T. L.,
- 1652 Cook, B. I., Cruz, C. A., Del Genio, A. D., Elsaesser, G. S., Faluvegi, G., Kiang, N. Y., Kim, D., Lacis,
- 1653 A. A., Leboissetier, A., LeGrande, A. N., Lo, K. K., Marshall, J., Matthews, E. E., McDermid, S.,
- 1654 Mezuman, K., Murray, L. T., Oinas, V., Orbe, C., Pérez García-Pando, C., Perlwitz, J. P., Puma, M.
- 1655 J., Rind, D., Romanou, A., Shindell, D. T., Sun, S., Tausnev, N., Tsigaridis, K., Tselioudis, G., Weng,
- 1656 E., Wu, J., and Yao, M.-S.: CMIP6 Historical Simulations (1850–2014) With GISS-E2.1, Journal of
- Advances in Modeling Earth Systems, 13, e2019MS002034,
- 1658 <u>https://doi.org/10.1029/2019MS002034, 2021.</u>
- 1659 Milly, P. C. D. and Dunne, K. A.: Potential evapotranspiration and continental drying, Nature Clim
- 1660 Change, 6, 946–949, https://doi.org/10.1038/nclimate3046, 2016.
- 1661 Minnis, P., Harrison, E. F., Stowe, L. L., Gibson, G. G., Denn, F. M., Doelling, D. R., and Smith, W.
- 1662 L.: Radiative Climate Forcing by the Mount Pinatubo Eruption, Science, 259, 1411–1415,
- 1663 https://doi.org/10.1126/science.259.5100.1411, 1993.
- 1664 Mintz, Y. and Walker, G. K.: Global Fields of Soil Moisture and Land Surface Evapotranspiration
- 1665 Derived from Observed Precipitation and Surface Air Temperature, 1993.
- Mullapudi, A., Vibhute, A. D., Mali, S., and Patil, C. H.: A review of agricultural drought
- assessment with remote sensing data: methods, issues, challenges and opportunities, Appl
- 1668 Geomat, 15, 1–13, https://doi.org/10.1007/s12518-022-00484-6, 2023.
- 1669 Myneni, R. B., Hoffman, S., Knyazikhin, Y., Privette, J. L., Glassy, J., Tian, Y., Wang, Y., Song, X.,
- 1670 Zhang, Y., Smith, G. R., Lotsch, A., Friedl, M., Morisette, J. T., Votava, P., Nemani, R. R., and
- 1671 Running, S. W.: Global products of vegetation leaf area and fraction absorbed PAR from year one
- of MODIS data, Remote Sensing of Environment, 83, 214–231, https://doi.org/10.1016/S0034-
- 1673 <u>4257(02)00074-3, 2002.</u>
- 1674 Narasimhan, B. and Srinivasan, R.: Development and evaluation of Soil Moisture Deficit Index
- 1675 (SMDI) and Evapotranspiration Deficit Index (ETDI) for agricultural drought monitoring,
- 1676 Agricultural and Forest Meteorology, 133, 69–88,
- 1677 https://doi.org/10.1016/j.agrformet.2005.07.012, 2005.

- 1678 <u>Neely III, R. R. and Schmidt, A.: VolcanEESM: Global volcanic sulphur dioxide (SO2) emissions</u>
- 1679 <u>database from 1850 to present Version 1.0 (1.0), https://doi.org/10.5285/76EBDC0B-0EED-</u>
- 1680 <u>4F70-B89E-55E606BCD568, 2016.</u>
- 1681 Nemani, R. R., Keeling, C. D., Hashimoto, H., Jolly, W. M., Piper, S. C., Tucker, C. J., Myneni, R. B.,
- 1682 and Running, S. W.: Climate-Driven Increases in Global Terrestrial Net Primary Production from
- 1683 1982 to 1999, Science, 300, 1560–1563, https://doi.org/10.1126/science.1082750, 2003.
- 1684 Nilson, S. E. and Assmann, S. M.: The Control of Transpiration. Insights from Arabidopsis, Plant
- 1685 Physiol, 143, 19–27, https://doi.org/10.1104/pp.106.093161, 2007.
- 1686 Olesen, J. E. and Bindi, M.: Consequences of climate change for European agricultural
- 1687 productivity, land use and policy, European Journal of Agronomy, 16, 239–262,
- 1688 https://doi.org/10.1016/S1161-0301(02)00004-7, 2002.
- 1689 Paik, S., Min, S.-K., Iles, C. E., Fischer, E. M., and Schurer, A. P.: Volcanic-induced global monsoon
- drying modulated by diverse El Niño responses, Science Advances, 6, eaba1212,
- 1691 https://doi.org/10.1126/sciadv.aba1212, 2020.
- 1692 Palmer, W. C.: Keeping Track of Crop Moisture Conditions, Nationwide: The New Crop Moisture
- 1693 Index, Weatherwise, 21, 156–161, https://doi.org/10.1080/00431672.1968.9932814, 1968.
- Pan, F., Nieswiadomy, M., and Qian, S.: Application of a soil moisture diagnostic equation for
- 1695 estimating root-zone soil moisture in arid and semi-arid regions, Journal of Hydrology, 524, 296–
- 1696 <u>310, https://doi.org/10.1016/j.jhydrol.2015.02.044, 2015.</u>
- 1697 Parker, D. E., Wilson, H., Jones, P. D., Christy, J. R., and Folland, C. K.: The Impact of Mount
- 1698 <u>Pinatubo on World-Wide Temperatures, International Journal of Climatology, 16, 487–497,</u>
- 1699 https://doi.org/10.1002/(SICI)1097-0088(199605)16:5<487::AID-JOC39>3.0.CO;2-J, 1996.
- 1700 Polvani, L. M., Banerjee, A., and Schmidt, A.: Northern Hemisphere continental winter warming
- following the 1991 Mt. Pinatubo eruption: reconciling models and observations, Atmospheric
- 1702 <u>Chemistry and Physics, 19, 6351–6366, https://doi.org/10.5194/acp-19-6351-2019, 2019.</u>
- 1703 Proctor, J., Hsiang, S., Burney, J., Burke, M., and Schlenker, W.: Estimating global agricultural
- 1704 effects of geoengineering using volcanic eruptions, Nature, 560, 480–483,
- 1705 https://doi.org/10.1038/s41586-018-0417-3, 2018.
- 1706 Ramachandran, S., Ramaswamy, V., Stenchikov, G. L., and Robock, A.: Radiative impact of the
- 1/707 Mount Pinatubo volcanic eruption: Lower stratospheric response, Journal of Geophysical
- 1708 Research: Atmospheres, 105, 24409–24429, https://doi.org/10.1029/2000JD900355, 2000.
- 1709 Robock, A.: Volcanic eruptions and climate, Reviews of Geophysics, 38, 191–219,
- 1710 <u>https://doi.org/10.1029/1998RG000054, 2000.</u>

- 1/711 Robock, A.: Cooling following large volcanic eruptions corrected for the effect of diffuse
- 1712 <u>radiation on tree rings, Geophysical Research Letters, 32,</u>
- 1713 https://doi.org/10.1029/2004GL022116, 2005.
- 1714 Robock, A. and Liu, Y.: The Volcanic Signal in Goddard Institute for Space Studies Three-
- 1715 Dimensional Model Simulations, Journal of Climate, 7, 44–55, https://doi.org/10.1175/1520-
- 1716 0442(1994)007<0044:TVSIGI>2.0.CO;2, 1994.
- 1717 Rogers, H. L., Norton, W. A., Lambert, A., and Grainger, R. G.: Transport of Mt. Pinatubo aerosol
- 1718 by tropospheric synoptic-scale and stratospheric planetary-scale waves, Quarterly Journal of the
- 1719 Royal Meteorological Society, 124, 193–209, https://doi.org/10.1002/qj.49712454509, 1998.
- 1720 Rosenzweig, C. and Abramopoulos, F.: Land-Surface Model Development for the GISS GCM,
- 1721 Journal of Climate, 10, 2040–2054, https://doi.org/10.1175/1520-
- 1722 0442(1997)010<2040:LSMDFT>2.0.CO;2, 1997.
- 1723 Rosenzweig, C. and Parry, M. L.: Potential impact of climate change on world food supply,
- 1724 Nature, 367, 133–138, https://doi.org/10.1038/367133a0, 1994.
- 1725 Sato, M., Hansen, J. E., McCormick, M. P., and Pollack, J. B.: Stratospheric aerosol optical depths,
- 1726 <u>1850–1990, Journal of Geophysical Research: Atmospheres, 98, 22987–22994,</u>
- 1727 https://doi.org/10.1029/93JD02553, 1993.
- 1728 Scheff, J. and Frierson, D. M. W.: Terrestrial Aridity and Its Response to Greenhouse Warming
- 1729 <u>across CMIP5 Climate Models, https://doi.org/10.1175/JCLI-D-14-00480.1, 2015.</u>
- 1730 Seneviratne, S. I., Corti, T., Davin, E. L., Hirschi, M., Jaeger, E. B., Lehner, I., Orlowsky, B., and
- 1731 <u>Teuling, A. J.: Investigating soil moisture–climate interactions in a changing climate: A review,</u>
- 1/32 Earth-Science Reviews, 99, 125–161, https://doi.org/10.1016/j.earscirev.2010.02.004, 2010.
- 1733 Sheng, J.-X., Weisenstein, D. K., Luo, B.-P., Rozanov, E., Arfeuille, F., and Peter, T.: A perturbed
- 1734 parameter model ensemble to investigate Mt. Pinatubo's 1991 initial sulfur mass emission,
- 1735 <u>Atmospheric Chemistry and Physics, 15, 11501–11512, https://doi.org/10.5194/acp-15-11501-</u>
- 1736 <u>2015, 2015a.</u>
- 1737 Sheng, J.-X., Weisenstein, D. K., Luo, B.-P., Rozanov, E., Stenke, A., Anet, J., Bingemer, H., and
- 1738 Peter, T.: Global atmospheric sulfur budget under volcanically quiescent conditions: Aerosol-
- <u>1739</u> <u>chemistry-climate model predictions and validation, Journal of Geophysical Research:</u>
- 1740 Atmospheres, 120, 256–276, https://doi.org/10.1002/2014JD021985, 2015b.
- 1741 <u>Shindell, D. T.: Climate and ozone response to increased stratospheric water vapor, Geophysical</u>
- 1742 Research Letters, 28, 1551–1554, https://doi.org/10.1029/1999GL011197, 2001.
- 1743 <u>Shindell, D. T., Faluvegi, G., and Bell, N.: Preindustrial-to-present-day radiative forcing by</u>
- 1744 tropospheric ozone from improved simulations with the GISS chemistry-climate GCM,

- 1745 <u>Atmospheric Chemistry and Physics, 3, 1675–1702, https://doi.org/10.5194/acp-3-1675-2003,</u>
- 1746 <u>2003.</u>
- 1747 Shindell, D. T., Faluvegi, G., Unger, N., Aguilar, E., Schmidt, G. A., Koch, D. M., Bauer, S. E., and
- Miller, R. L.: Simulations of preindustrial, present-day, and 2100 conditions in the NASA GISS
- 1749 composition and climate model G-PUCCINI, Atmospheric Chemistry and Physics, 6, 4427–4459,
- 1750 https://doi.org/10.5194/acp-6-4427-2006, 2006.
- 1751 Simard, M., Pinto, N., Fisher, J. B., and Baccini, A.: Mapping forest canopy height globally with
- 1752 spaceborne lidar, Journal of Geophysical Research: Biogeosciences, 116,
- 1753 <u>https://doi.org/10.1029/2011JG001708, 2011.</u>
- 1754 Singh, R. and AchutaRao, K.: Quantifying uncertainty in twenty-first century climate change over
- 1755 India, Clim Dyn, 52, 3905–3928, https://doi.org/10.1007/s00382-018-4361-6, 2019.
- 1756 Singh, R., Tsigaridis, K., LeGrande, A. N., Ludlow, F., and Manning, J. G.: Investigating
- 1757 <u>hydroclimatic impacts of the 168–158 BCE volcanic quartet and their relevance to the</u>
- 1758 <u>Nile River basin and Egyptian history, Climate of the Past, 19, 249–275,</u>
- 1759 https://doi.org/10.5194/cp-19-249-2023, 2023.
- 1760 Stenchikov, G. L., Kirchner, I., Robock, A., Graf, H.-F., Antuña, J. C., Grainger, R. G., Lambert, A.,
- and Thomason, L.: Radiative forcing from the 1991 Mount Pinatubo volcanic eruption, Journal
- 1762 of Geophysical Research: Atmospheres, 103, 13837–13857,
- 1763 https://doi.org/10.1029/98JD00693, 1998.
- 1764 Tejedor, E., Steiger, N. J., Smerdon, J. E., Serrano-Notivoli, R., and Vuille, M.: Global hydroclimatic
- 1765 response to tropical volcanic eruptions over the last millennium, Proceedings of the National
- 1766 Academy of Sciences, 118, e2019145118, https://doi.org/10.1073/pnas.2019145118, 2021.
- 1767 <u>Thornthwaite, C. W.: An Approach toward a Rational Classification of Climate, Geographical</u>
- 1768 Review, 38, 55–94, https://doi.org/10.2307/210739, 1948.
- 1769 <u>Timmreck, C.: Modeling the climatic effects of large explosive volcanic eruptions, WIREs Climate</u>
- 1770 Change, 3, 545–564, https://doi.org/10.1002/wcc.192, 2012.
- 1771 Timmreck, C., Graf, H.-F., and Feichter, J.: Simulation of Mt. Pinatubo Volcanic Aerosol with the
- 1772 Hamburg Climate Model ECHAM4, Theor Appl Climatol, 62, 85–108,
- 1773 https://doi.org/10.1007/s007040050076, 1999.
- 1774 Toohey, M., Krüger, K., Sigl, M., Stordal, F., and Svensen, H.: Climatic and societal impacts of a
- 1775 <u>volcanic double event at the dawn of the Middle Ages, Climatic Change, 136, 401–412,</u>
- 1776 https://doi.org/10.1007/s10584-016-1648-7, 2016.
- 1777 Toohey, M., Krüger, K., Schmidt, H., Timmreck, C., Sigl, M., Stoffel, M., and Wilson, R.:
- 1778 <u>Disproportionately strong climate forcing from extratropical explosive volcanic eruptions,</u>
- 1779 Nature Geosci, 12, 100–107, https://doi.org/10.1038/s41561-018-0286-2, 2019.

- 1780 <u>Trenberth, K. E. and Dai, A.: Effects of Mount Pinatubo volcanic eruption on the hydrological</u>
- 1781 cycle as an analog of geoengineering, Geophysical Research Letters, 34,
- 1782 https://doi.org/10.1029/2007GL030524, 2007.
- 1783 Trenberth, K. E. and Stepaniak, D. P.: The flow of energy through the earth's climate system,
- 1784 <u>Quarterly Journal of the Royal Meteorological Society, 130, 2677–2701,</u>
- 1785 https://doi.org/10.1256/qj.04.83, 2004.
- 1786 Trenberth, K. E., Fasullo, J. T., and Kiehl, J.: Earth's Global Energy Budget, Bulletin of the
- 1787 American Meteorological Society, 90, 311–324, https://doi.org/10.1175/2008BAMS2634.1,
- 1788 2009.
- 1789 Trepte, C. R., Veiga, R. E., and McCormick, M. P.: The poleward dispersal of Mount Pinatubo
- 1790 volcanic aerosol, Journal of Geophysical Research: Atmospheres, 98, 18563–18573,
- 1791 https://doi.org/10.1029/93JD01362, 1993.
- 1792 <u>Vehkamäki, H., Kulmala, M., Napari, I., Lehtinen, K. E. J., Timmreck, C., Noppel, M., and</u>
- 1793 <u>Laaksonen, A.: An improved parameterization for sulfuric acid–water nucleation rates for</u>
- 1794 tropospheric and stratospheric conditions, Journal of Geophysical Research: Atmospheres, 107,
- 1795 AAC 3-1-AAC 3-10, https://doi.org/10.1029/2002JD002184, 2002.
- 1796 <u>Wada, Y., Wisser, D., Eisner, S., Flörke, M., Gerten, D., Haddeland, I., Hanasaki, N., Masaki, Y.,</u>
- 1797 Portmann, F. T., Stacke, T., Tessler, Z., and Schewe, J.: Multimodel projections and uncertainties
- 1798 of irrigation water demand under climate change, Geophysical Research Letters, 40, 4626–4632,
- 1799 https://doi.org/10.1002/grl.50686, 2013.
- Weng, E., Aleinov, I., Singh, R., Puma, M. J., McDermid, S. S., Kiang, N. Y., Kelley, M., Wilcox, K.,
- 1801 Dybzinski, R., Farrior, C. E., Pacala, S. W., and Cook, B. I.: Modeling demographic-driven
- 1802 vegetation dynamics and ecosystem biogeochemical cycling in NASA GISS's Earth system
- 1803 model (ModelE-BiomeE v.1.0), Geoscientific Model Development Discussions, 1–60,
- 1804 <u>https://doi.org/10.5194/gmd-2022-72, 2022.</u>
- 1805 van der Werf, G. R., Randerson, J. T., Giglio, L., van Leeuwen, T. T., Chen, Y., Rogers, B. M., Mu,
- 1806 M., van Marle, M. J. E., Morton, D. C., Collatz, G. J., Yokelson, R. J., and Kasibhatla, P. S.: Global
- fire emissions estimates during 1997–2016, Earth System Science Data, 9, 697–720,
- 1808 <u>https://doi.org/10.5194/essd-9-697-2017, 2017.</u>
- 1809 Wisser, D., Fekete, B. M., Vörösmarty, C. J., and Schumann, A. H.: Reconstructing 20th century
- 1810 global hydrography: a contribution to the Global Terrestrial Network- Hydrology (GTN-H),
- 1811 Hydrology and Earth System Sciences, 14, 1–24, https://doi.org/10.5194/hess-14-1-2010, 2010.
- 1812 Zuo, M., Zhou, T., and Man, W.: Hydroclimate Responses over Global Monsoon Regions
- Following Volcanic Eruptions at Different Latitudes, https://doi.org/10.1175/JCLI-D-18-0707.1,
- 1814 <u>2019a.</u>

Zuo, M., Zhou, T., and Man, W.: Wetter Global Arid Regions Driven by Volcanic Eruptions, Journal of Geophysical Research: Atmospheres, 124, 13648–13662, https://doi.org/10.1029/2019JD031171, 2019b.